Electronic Supplementary Information

One-step synthesis of perylenediimides exhibiting near-infrared absorption and emission by amino-yne click reaction

Haruki Sanematsu[ab], Masayuki Takeuchi[ab] and Atsuro Takai*[a]

[a] Molecular Design and Function Group, National Institute for Materials Science (NIMS), 1-2-1 Sengen, Tsukuba, Ibaraki 305-0047, Japan

[b] Department of Materials Science and Engineering, Faculty of Pure and Applied Sciences, University of Tsukuba, 1-1-1 Tennodai, Tsukuba, Ibaraki 305-8577, Japan

Table of Contents	

Experimental Methods

Abbreviations of chemical names:

$CHCl_3$	chloroform
$CDCl_3$	chloroform-*d*
TMS	tetramethylsilane (in NMR data) or trimethylsilyl (in others)
NMP	*N*-methylpyrrolidone
AcOH	acetic acid
THF	tetrahydrofuran
MeOH	methanol
DME	1,2-dimethoxyethane
MeCN	acetonitrile

Materials: All reagents and solvents were purchased from Tokyo Chemical Industry Co., Kanto Chemical Co., FUJIFILM Wako Pure Chemical Corporation or Sigma-Aldrich Co. and used without further purification. The target compounds were purified by a recycling preparative HPLC (JAI LaboACE LC-5060) equipped with a gel permeation chromatography column (YMC-GPC T4000) using $CHCl_3$ as an eluent.

Nuclear magnetic resonance (NMR) spectroscopy: ^{1}H NMR (400 MHz) and ^{13}C NMR (101 MHz) spectra were recorded by a JEOL ECS-400 spectrometer. Tetramethylsilane (TMS; 0 ppm) was used as an internal standard.

UV-vis-NIR absorption spectroscopy: UV-vis-NIR absorption spectra were recorded by a JASCO V-670 and V-730 spectrophotometers, equipped with a Peltier temperature controller. The optical path length for solution samples was 1 cm. The time course of reactions was measured with a time-interval measurement mode while stirring the solution at 600 r.p.m. UV-vis-NIR reflection spectra of solid samples were measured using an integrating sphere attachment in diffuse reflection mode.

Fluorescence spectroscopy: Fluorescence and excitation spectra in the NIR region were recorded by a HORIBA NanoLog spectrophotometer using a 450 W xenon arc lamp as the

excitation source. A cut-on filter for 500 nm-light was used to avoid scattered excitation light. The optical path length for solution samples was 1 cm. The excitation wavelength was selected so that the absorbance in each solvent was similar around 0.7. Absolute fluorescence quantum yields were obtained on a Hamamatsu Photonics C11347-02.

Fluorescence lifetime measurements: Fluorescence lifetime of the PDI derivatives were measured by a Horiba FluoroCube time-correlated single-photon-counting system equipped with a pulse laser at 375 nm (PicoBrite) with a solution of LUDOX HS-30 scatterer as a reference. The decay profile simulations were performed by a nonlinear least-squares method.

Mass spectrometry: High-resolution mass spectrometry was performed with a Bruker micrOTOF II mass spectrometer, equipped with an atmospheric pressure chemical ionization source (APCI TOF–MS). Isotopic distribution pattern was calculated using an iMass 1.6 software.

Quantum chemical calculation: Density functional theory (DFT) and time-dependent DFT (TDDFT) calculations were carried out with a Gaussian 16, Revision C.01 software.[S1] Optimized structures in the ground state and the excited state were obtained by DFT and TDDFT at the CAM-B3LYP/6-31+g(d) level, respectively. The graphics were drawn using a Gauss View software program (version 6.1) developed by Semichem Inc.[S2]

Thermal analysis: Differential scanning calorimetry (DSC) was carried out on a NETZSCH DSC 3500 Sirius under nitrogen atmosphere. The sample was encapsulated in a sealed aluminum pan, and an identical empty pan was used as the reference. The DSC data were obtained during the second heating/cooling cycles at a scan rate of 10 K/min. Thermogravimetric analysis (TGA) was conducted with a NETZSCH STA2500 Regulus at a heating rate of 10 K/min under flowing nitrogen gas. The sample was placed in an aluminum pan.

Synthesis and Characterization

Synthetic overview of ***o*-ePDI1**, ***b*-ePDI1**, and ***b*-ePDI2** are shown in Scheme S1. We employed *N*,*N*'-bis(3-pentyl)perylenediimide (PDI) as a starting compound due to its high solubility and stability in various organic solvents. Bromination at the *bay*- and *ortho*-positions was attained by direct bromination with Br_2 and Ir-catalyzed boronation followed by bromination with $CuBr_2$, respectively. Sonogashira coupling reaction of the brominated PDIs with trimethylsilylacetylene then afforded TMS-protected ethynyl PDIs. Finally, the TMS group was cleaved with base to give ethynyl PDIs (***o*-ePDI1**, ***b*-ePDI1**). Diethynyl PDI (***b*-ePDI2**) should be obtained in a similar manner; alternatively, ***b*-ePDI2** was also obatined in one step by Stille coupling reaction of the dibromo PDI with tri(*n*-butyl)ethynylltin, although the reaction yield was low. The individual synthetic protocols are described below.

Scheme S1 Synthetic scheme of ***b*-ePDI1**, ***o*-ePDI1**, and ***b*-ePDI2**.

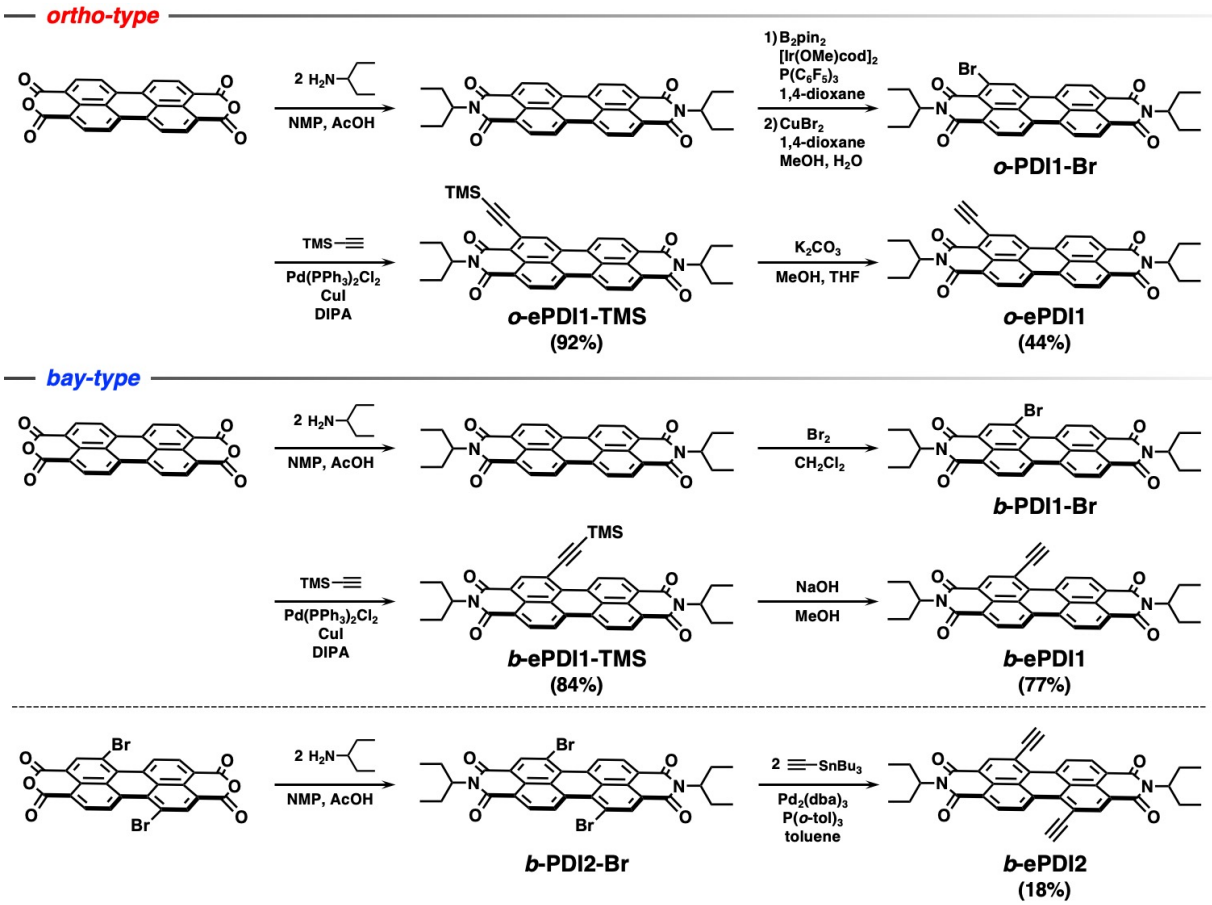

Synthesis of *o*-ePDI1-TMS:

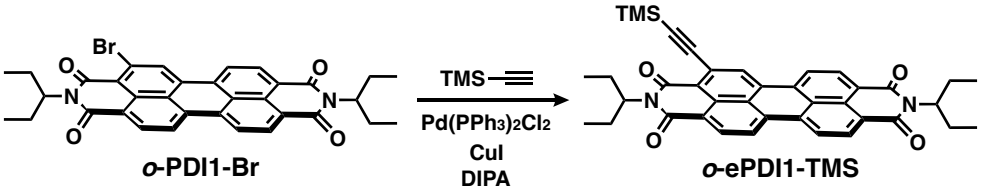

***o*-PDI1-Br** was synthesized according to the literature.[S3] Under argon atmosphere, ***o*-ePDI1-Br** (245 mg, 0.40 mmol), trimethylsilylacetylene (140 μL, 1.02 mmol), bis(triphenylphosphine)palladium dichloride ($Pd(PPh_3)_2Cl_2$; 71 mg, 0.1 mmol), and CuI (19 mg, 10 μmol) were stirred in degassed diisopropylamine (DIPA, 12 mL) for 30 min at 318 K. The reaction mixture was cooled to room temperature (r.t.) and filtrated through a Celite eluting with CH_2Cl_2. The solvents were removed under reduced pressure, and the crude was purified by silica-gel column chromatography using CH_2Cl_2 as an eluent. The red solid was further purified by reprecipitation from CH_2Cl_2 and MeOH to afford ***o*-ePDI1-TMS** as a red solid (230 mg, 92%).

^{1}H NMR (400 MHz, $CDCl_3$): δ (ppm) = 0.42 (s, 9H), 0.93 (td, J = 7.5, 2.2 Hz, 12H), 1.89–2.02 (m, 4H), 2.20–2.33 (m, 4H), 5.03–5.11 (m, 2H), 8.60–8.71 (m, 7H). ^{13}C NMR (101 MHz, $CDCl_3$): δ (ppm) = 0.13, 11.49, 11.58, 25.08, 25.16, 57.85, 104.63, 107.33, 123.19, 123.36, 123.38, 123.63 (br), 124.17 (br), 125.93, 126.55, 127.22 (br), 129.70, 129.82, 130.24, 131.66 (br), 131.90 (br), 133.29, 133.93, 134.30, 134.65, 163.98 (br). APCI TOF–MS: calcd. for $C_{39}H_{38}N_2O_4Si$; $[M]^-$ 626.2606; found: 626.2629.

Synthesis of *o*-ePDI1:

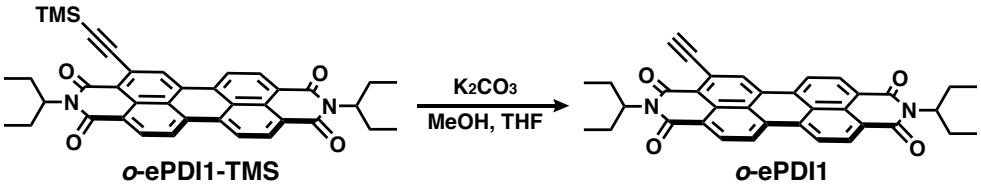

Under argon atmosphere, ***o*-ePDI1-TMS** (124 mg, 0.20 mmol) and K_2CO_3 (16 mg, 0.12 mmol) were stirred in a mixture of dry THF and MeOH (12 mL, w/w = 1/1) for 10 min at r.t. The solvents were removed under reduced pressure, and the crude was purified by silica-gel column chromatography using CH_2Cl_2 as an eluent. The red solid was further purified by recycling HPLC to afford ***o*-ePDI1** as a red solid (48 mg, 44%).

^{1}H NMR (400 MHz, $CDCl_3$): δ (ppm) = 0.94 (td, J = 7.5, 2.0 Hz, 12H), 1.90–2.03 (m, 4H), 2.21–2.33 (m, 4H), 3.94 (s, 1H), 5.03–5.13 (m, 2H), 8.61–8.64 (m, 3H), 8.67–8.73 (m, 4H). ^{13}C NMR (101 MHz, $CDCl_3$): δ (ppm) = 11.37, 11.44, 24.93, 25.02, 57.77, 57.94, 83.35, 87.93, 123.19, 123.27, 123.38, 123.97 (br), 125.95, 126.30, 129.50, 129.66, 130.03, 131.45

(br), 131.97 (br), 133.45, 133.51, 134.22, 134.27, 163.56 (br). APCI TOF–MS: calcd. for $C_{36}H_{30}N_2O_4$; $[M]^-$ 554.2211; found: 554.2225.

Synthesis of *o*-ePDI1–DBA:

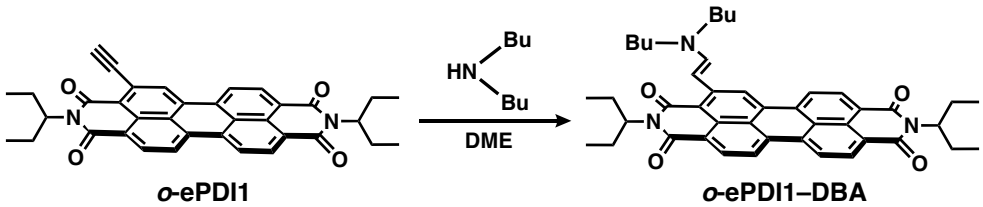

***o*-ePDI1** (10 mg, 18 μmol) was dissolved in dehydrated DME (3 mL). Then, dibutylamine (**DBA**; 40 μL) was added and the reaction mixture was stirred for 1 h at 295 K. The solvent and unreacted amine were removed under reduced pressure, and the obtained solid was purified by recycling HPLC to afford ***o*-ePDI1–DBA** as a dark reddish purple solid (12 mg, 97%).

^{1}H NMR (400 MHz, $CDCl_3$): δ (ppm) = 0.93 (td, J = 7.5, 4.9 Hz, 12H), 1.03 (t, J = 7.4 Hz, 6H), 1.43–1.52 (m, 4H), 1.70–1.78 (m, 4H), 1.89–2.00 (m, 4H), 2.22–2.34 (m, 4H), 3.42 (t, J = 7.5 Hz, 4H), 5.04–5.17 (m, 2H), 7.55 (d, J = 13.8 Hz, 1H), 7.60 (d, J = 13.8 Hz, 1H), 8.33 (d, J = 8.3 Hz, 1H), 8.52–8.60 (m, 3H), 8.63–8.68 (m, 3H). ^{13}C NMR (101 MHz, $CDCl_3$): δ (ppm) = 11.39, 11.49, 13.90, 20.25, 25.04, 25.11, 30.21 (br), 57.06 (br), 57.51, 96,90, 110.78, 119.67, 121.04, 121.66, 122.27, 122.61 (br), 123.14, 126.43, 129.53, 130.82, 131.51, 132.36, 132.99, 135.31, 135.62, 146.51, 146.52, 164.47 (br). APCI TOF–MS: m/z calcd. for $C_{44}H_{50}N_3O_4$; $[M+H]^+$ 684.3796; found: 684.3807.

Synthesis of *b*-ePDI1-TMS:

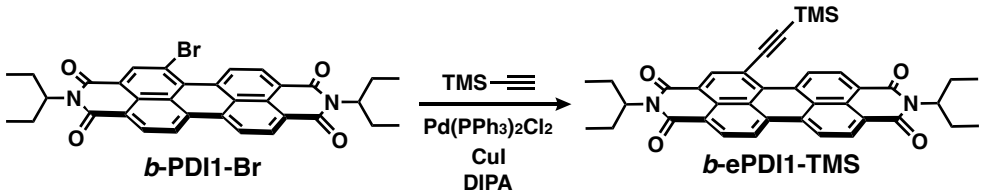

***b*-PDI1-Br** was synthesized according to the literature.[S4] Under argon atmosphere, ***b*-ePDI1-Br** (122 mg, 0.20 mmol), trimethylsilylacetylene (70 μL, 0.51 mmol), $Pd(PPh_3)_2Cl_2$ (35 mg, 50 μmol), and CuI (1.2 mg, 6.3 μmol) were stirred in degassed DIPA (6 mL) for 30 min at 318 K. The reaction mixture was cooled to r.t. and filtrated through a Celite eluting with CH_2Cl_2. The solvents were removed under reduced pressure, and the crude was purified by silica-gel column chromatography using CH_2Cl_2 as an eluent. The yellow solid was further purified by reprecipitation from CH_2Cl_2 and MeOH to afford ***b*-ePDI1-TMS** as a red solid (106 mg, 84%).

^{1}H NMR (400 MHz, $CDCl_3$): δ (ppm) = 0.41 (s, 9H), 0.93 (td, J = 7.5, 5.1 Hz, 12H), 1.88–2.00 (m, 4H), 2.21–2.34 (m, 4H), 5.02–5.12 (m, 4H), 8.65–8.71 (m, 5H), 8.81 (s, 1H), 10.39 (d, J = 8.3 Hz, 1H). ^{13}C NMR (101 MHz, $CDCl_3$): δ (ppm) = –0.38, 11.32, 11.36, 24.98, 25.05, 57.71, 57.80, 105.93, 107.26, 119.93, 122.28 (br), 123.01, 123.47, 123.69 (br), 126.66, 127.15, 127.20, 128.24, 128.67, 129.05, 129.12, 131.01 (br), 133.88, 134.27, 134.52, 134.61, 138.92 (br), 163.96 (br). APCI TOF–MS: calcd. for $C_{39}H_{38}N_2O_4Si$; $[M]^-$ 626.2606; found: 626.2622.

Synthesis of *b*-ePDI1:

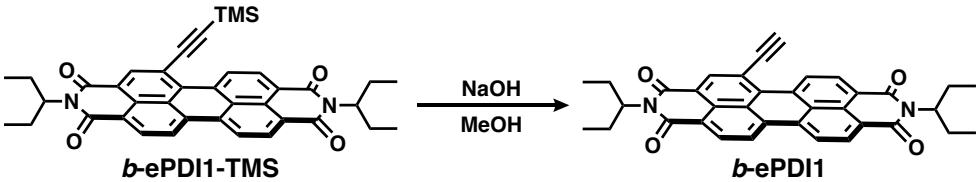

Under argon atmosphere, saturated NaOH solution of MeOH (0.7 mL) was added to a $CHCl_3$ (14 mL) solution of the ***b*-ePDI1-TMS** (96 mg, 0.15 mmol), and stirred for 5 min at 295 K. The product was extracted with $CHCl_3$ and washed by distilled water. The solvents were removed under reduced pressure, and the crude was purified by silica-gel column chromatography using CH_2Cl_2 as an eluent. The red solid was further purified by recycling HPLC and reprecipitation from CH_2Cl_2 and MeOH to afford ***b*-ePDI1** as a red solid (66 mg, 77%).

^{1}H NMR (400 MHz, $CDCl_3$): δ (ppm) = 0.93 (td, J = 7.4, 2.7 Hz, 12H), 1.89–2.00 (m, 4H), 2.21–2.33 (m, 4H), 3.94 (s, 1H), 5.02–5.11 (m, 2H), 8.66–8.72 (m, 5H), 8.83 (s, 1H), 10.27 (d, J = 8.3 Hz, 1H). ^{13}C NMR (101 MHz, $CDCl_3$): δ (ppm) = 11.34, 11.36, 24.97, 25.02, 57.72, 57.83, 84.64, 87.88, 118.77, 123.10, 123.49, 123.82 (br), 126.60, 127.13, 127.24, 128.84, 129.08, 131.29 (br), 133.75, 133.93, 134.55, 135.27, 139.09 (br), 164.00 (br). APCI TOF–MS: calcd. for $C_{36}H_{30}N_2O_4$; $[M]^-$ 554.2211; found: 554.2225.

Synthesis of *b*-ePDI1–DBA:

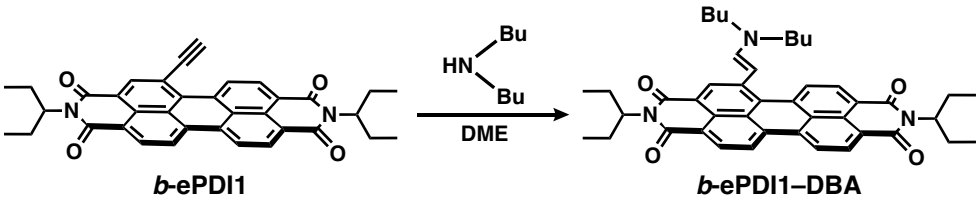

***b*-ePDI1** (10 mg, 18 μmol) was dissolved in dehydrated DME (5 mL). Then, **DBA** (50 μL) was added and the reaction mixture was stirred for 3 h at 294 K. The solvent and unreacted amine were removed under reduced pressure, and the obtained solid was purified by recycling HPLC to afford ***b*-ePDI1–DBA** as a dark green solid (12 mg, 91%).

^{1}H NMR (400 MHz, $CDCl_3$): δ (ppm) = 0.93 (td, J = 7.4, 1.4 Hz, 12H), 1.02 (t, J = 7.4 Hz, 6H), 1.37–1.47 (m, 4H), 1.64–1.71 (m, 4H), 1.87–1.99 (m, 4H), 2.22–2.34 (m, 4H), 3.27 (t, J = 7.5 Hz, 4H), 5.03–5.13 (m, 2H), 6.18 (d, J = 13.4 Hz, 1H), 7.52 (d, J = 13.4 Hz, 1H), 8.44–8.53 (m, 4H), 8.64 (d, J = 8.3 Hz, 1H), 8.66 (s, 1H), 9.09 (d, J = 8.3 Hz, 1H). ^{13}C NMR (101 MHz, $CDCl_3$): δ (ppm) = 11.33, 11.37, 14.03, 20.19, 20.24, 25.06, 25.11, 31.33, 52.31 (br), 57.38, 57.53, 98.70, 121.11, 123.63, 125.06, 125.30, 126.16, 127.93, 128.53, 129.84, 131.47 (br), 133.19, 135.25, 137.06, 140.84, 144.49, 164.73 (br). APCI TOF–MS: m/z calcd. for $C_{44}H_{49}N_3O_4$; $[M]^+$ 683.3718; found: 683.3705.

Synthesis of *b*-ePDI2:

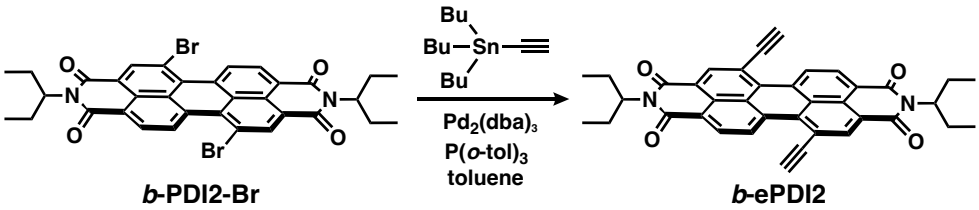

***b*-PDI2-Br** was synthesized according to established procedures of analogous compounds.[S5] Under argon atmosphere, ***b*-PDI2-Br** (275 mg, 0.4 mmol), tri(n-butyl)ethynyltin (0.27 mL, 0.94 mmol), tris(dibenzylideneacetone) dipalladium ($Pd_2(dba)_3$; 36 mg, 40 μmol), and tri(o-tolyl)phosphine (P(o-tol)$_3$; 24 mg, 0.17 mmol) were stirred in anhydrous toluene (25 mL) for 10 min at 295 K. The reaction mixture was cooled to r.t. and filtrated through a Celite eluting with CH_2Cl_2. The solvents were removed under reduced pressure, and the crude was purified by silica-gel column chromatography using CH_2Cl_2 as an eluent to afford ***b*-ePDI2** as a red solid (40 mg, 18%). The ^{13}C NMR spectrum could not be obtained even at higher temperatures or in other solvents due to the poor solubility of ***b*-ePDI2**.

^{1}H NMR (400 MHz, $CDCl_3$): δ (ppm) = 0.92 (t, J = 7.5 Hz, 12H), 1.89–1.99 (m, 4H), 2.21–2.32 (m, 4H), 3.82 (s, 1H), 5.02–5.10 (m, 2H), 8.71 (d, J = 8.2 Hz, 2H), 8.85 (s, 2H), 10.06 (d, J = 8.2 Hz, 2H). APCI TOF–MS: m/z calcd. for $C_{38}H_{30}N_2O_4$; $[M]^-$ 578.2211; found: 578.2196.

Synthesis of *b*-ePDI2–(DBA)$_2$:

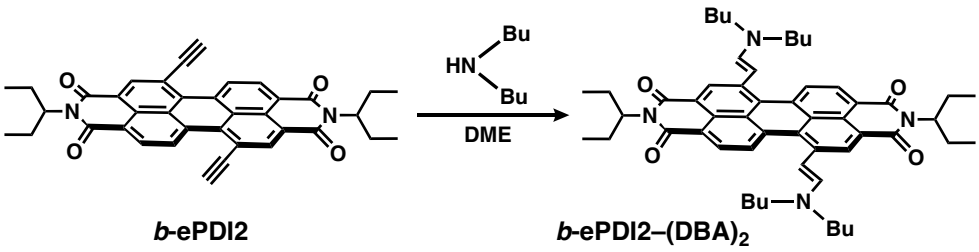

***b*-ePDI2** (20 mg, 0.035 mmol) was dissolved in dehydrated DME (10 mL). Then, **DBA** (1 mL) was added and the reaction mixture was stirred for 7 h at 295 K. The solvent and unreacted amine were removed under reduced pressure, and the obtained solid was purified by recycling HPLC to afford ***b*-ePDI2–(DBA)$_2$** as a green solid (25 mg, 85%).

^{1}H NMR (400 MHz, $CDCl_3$): δ (ppm) = 0.92 (t, J = 7.4 Hz, 12H), 1.00 (t, J = 7.3 Hz, 12H), 1.35–1.44 (m, 4H), 1.61–1.68 (m, 4H), 1.87–1.97 (m, 4H), 2.23–2.34 (m, 4H), 3.22 (t, J = 7.5 Hz, 8H), 5.05–5.13 (m, 2H), 6.05 (d, J = 13.6 Hz, 2H), 7.41 (d, J = 13.6 Hz, 2H), 8.30 (d, J = 8.2 Hz, 2H), 8.65 (s, 2H), 8.91 (d, J = 8.2 Hz, 2H). ^{13}C NMR (101 MHz, $CDCl_3$): δ (ppm) = 11.35, 14.05, 20.24, 25.13, 31.25, 52.07, 57.24, 98.08, 120.22 (br), 121.19 (br), 125.32, 126.11, 126.84 (br), 127.09, 129.87 (br), 130.13, 135.91, 138.42, 143.15, 165.08 (br). APCI TOF–MS: m/z calcd. for $C_{54}H_{69}N_4O_4$; $[M+H]^+$ 837.5313; found: 837.5271.

Synthesis of *b*-ePDI2–PEI:

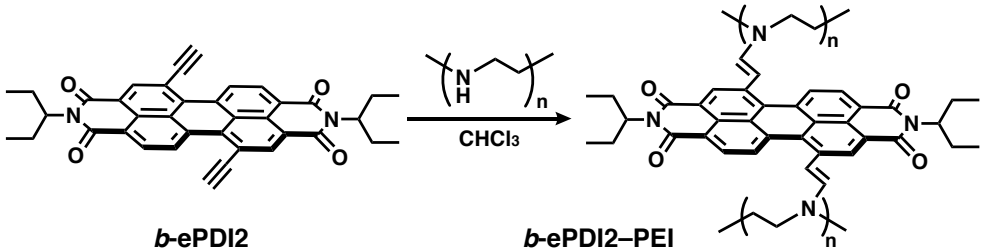

A linear polyethylenimine (**PEI**) with average M_n of 10 kDa was purchased from Sigma-Aldrich Co. To a $CHCl_3$ (12 mL) solution of **PEI** (86 mg) was added ***b*-ePDI2** (1.1 mg, 1.9 μmol), and the reaction mixture was stirred for 16 h at 294 K. The product was reprecipitated from $CHCl_3$ and hexane to afford ***b*-ePDI2–PEI** as an opaque green solid (78 mg).

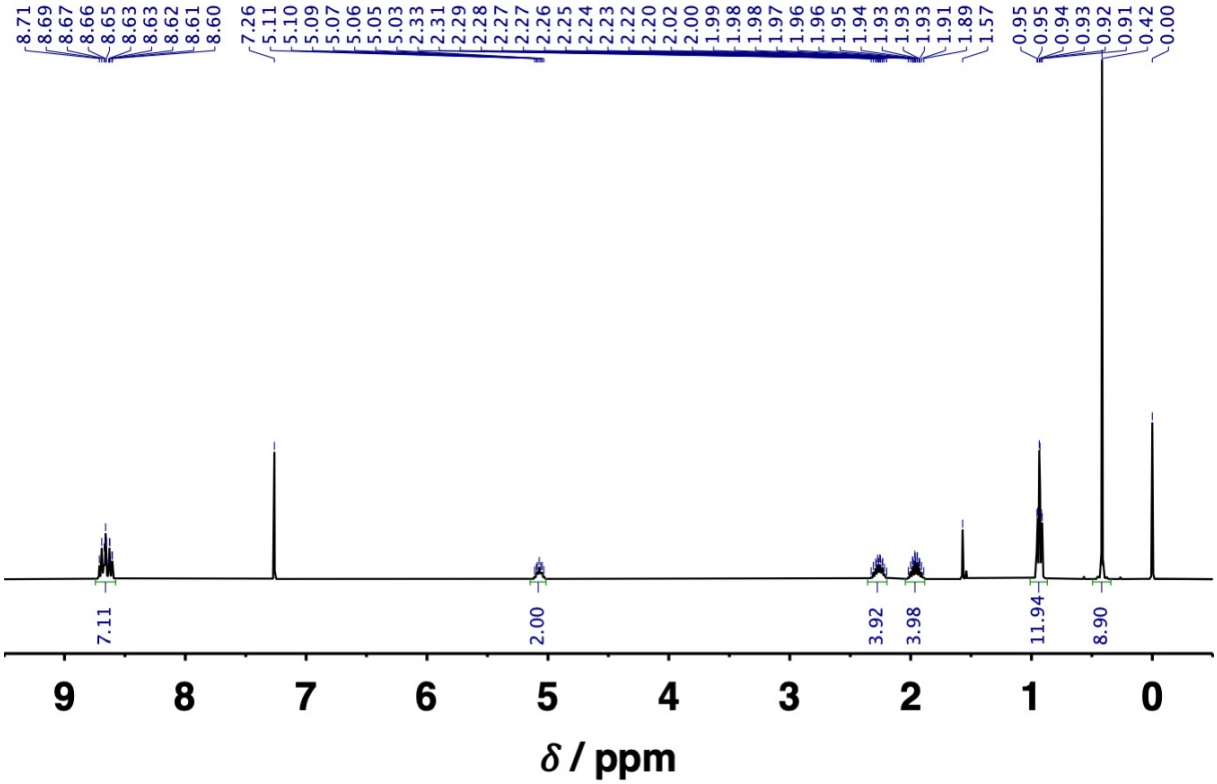

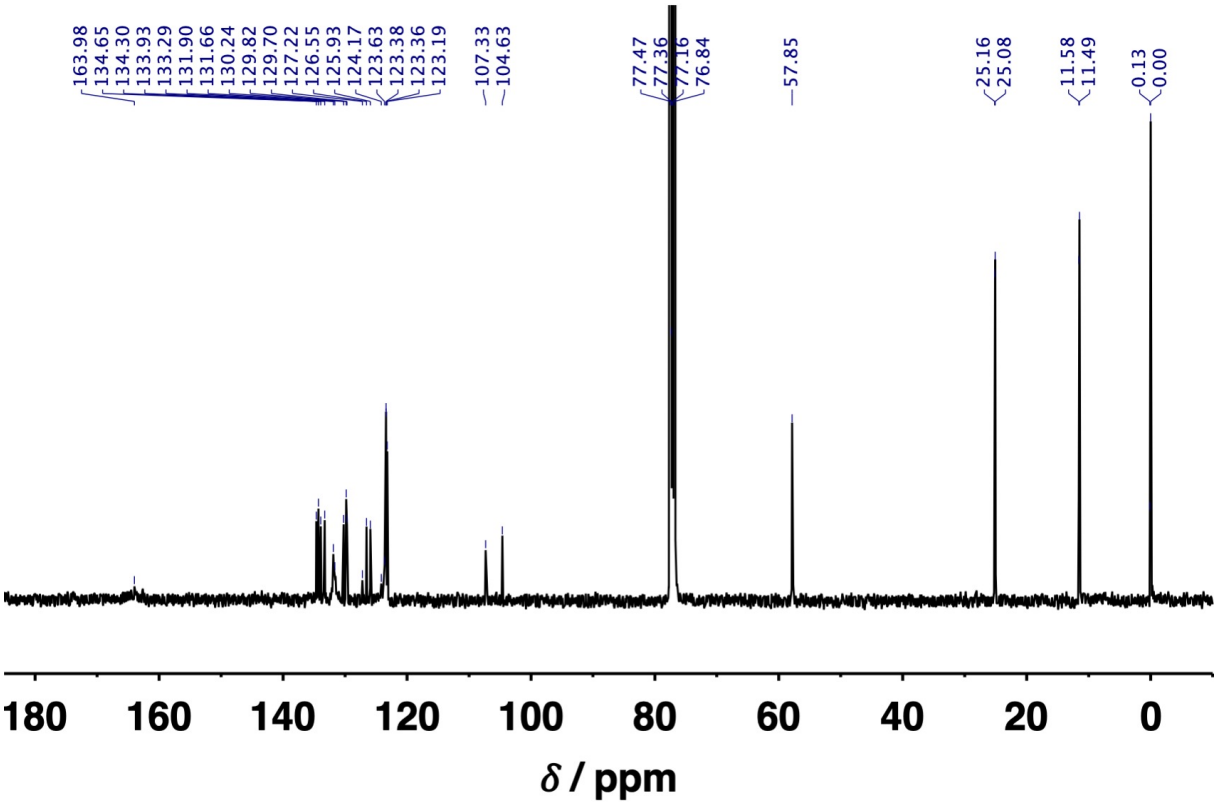

^{1}H NMR (top) and ^{13}C NMR (bottom) spectra of ***o*-ePDI1-TMS** in $CDCl_3$ at 298 K.

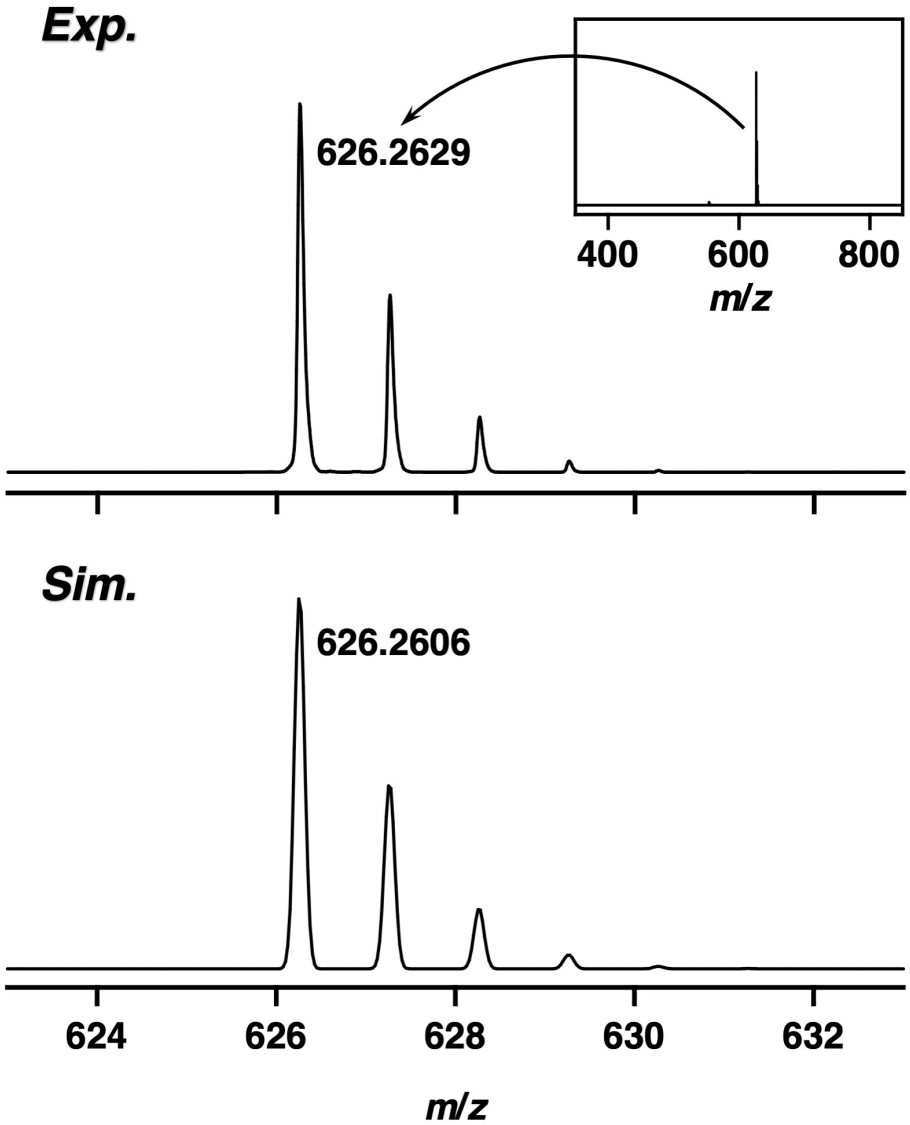

APCI TOF–MS chart of ***o*-ePDI1-TMS** (negative ion) and its calculated isotopic distribution (calcd. for $C_{39}H_{38}N_2O_4Si$; $[M]^-$).

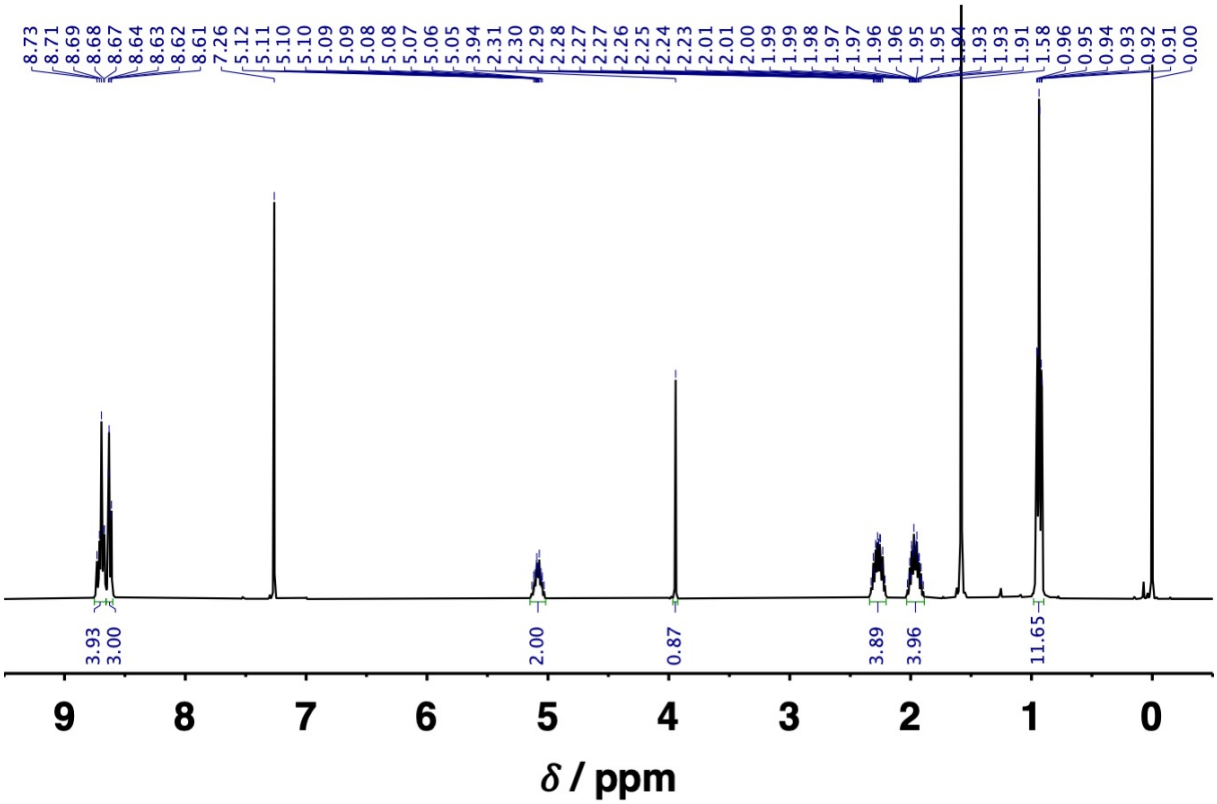

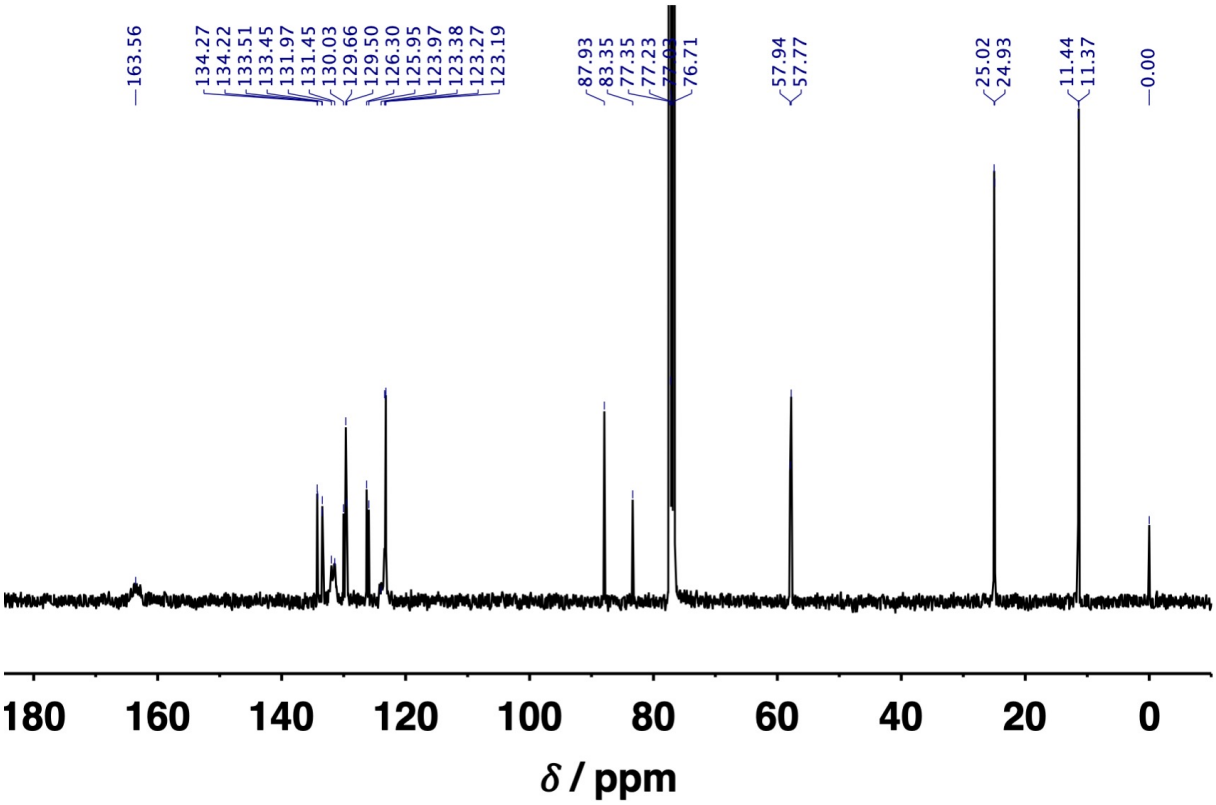

^{1}H NMR (top) and ^{13}C NMR (bottom) spectra of ***o*-ePDI1** in $CDCl_3$ at 298 K.

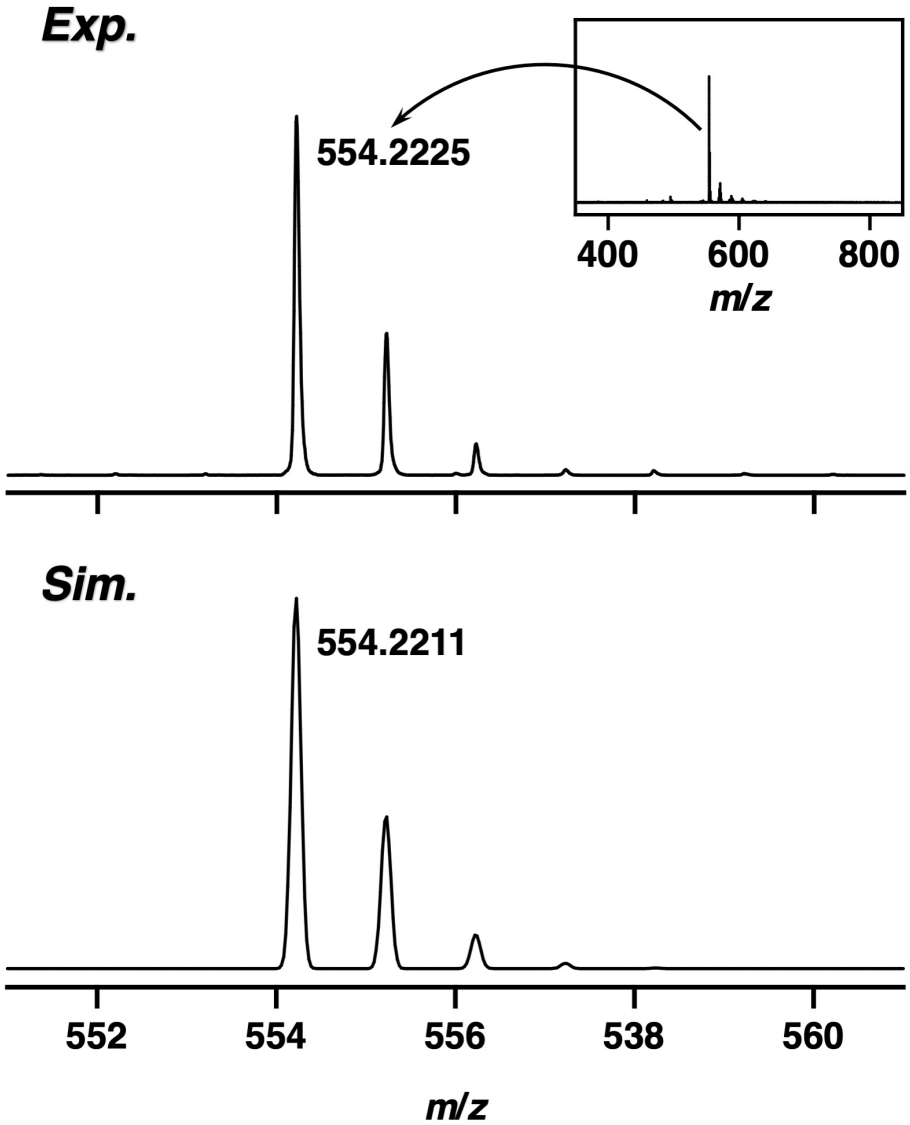

APCI TOF–MS chart of ***o*-ePDI1** (negative ion) and its calculated isotopic distribution (calcd. for $C_{36}H_{30}N_2O_4$; $[M]^-$).

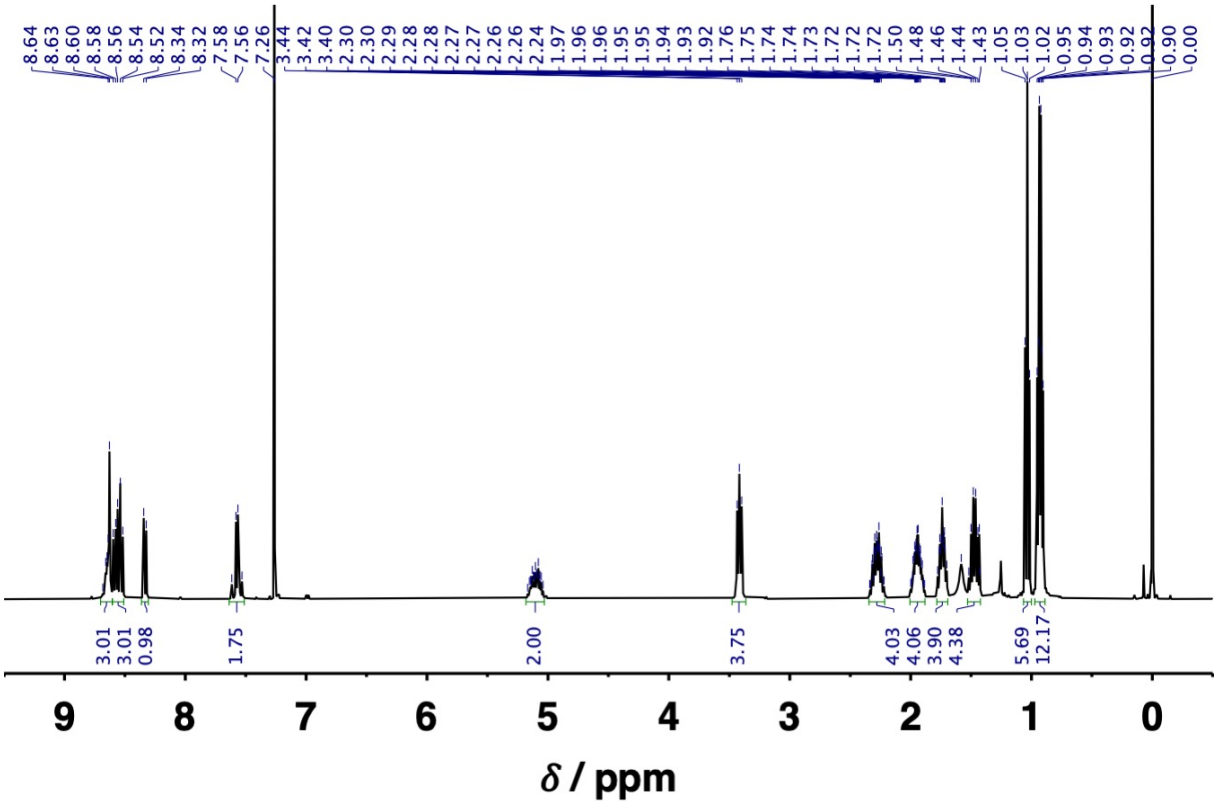

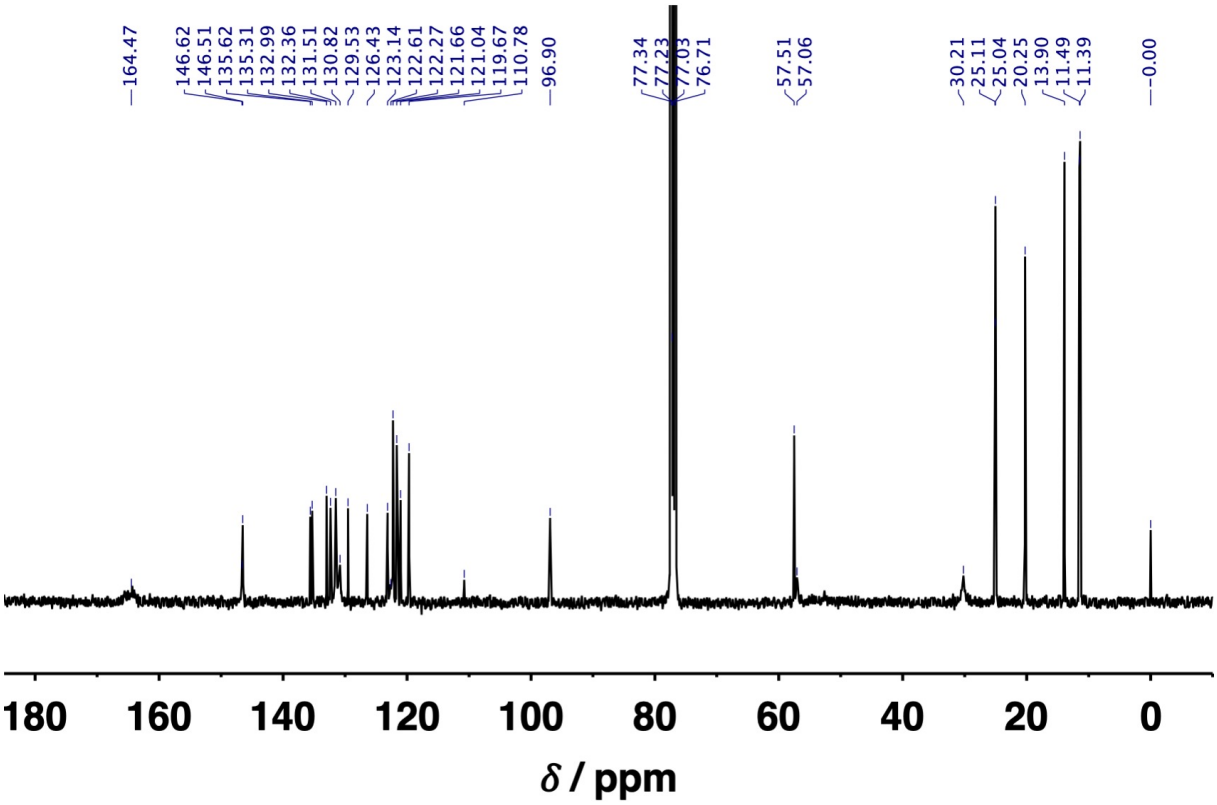

^{1}H NMR (top) and ^{13}C NMR (bottom) spectra of ***o*-ePDI1–DBA** in $CDCl_3$ at 298 K.

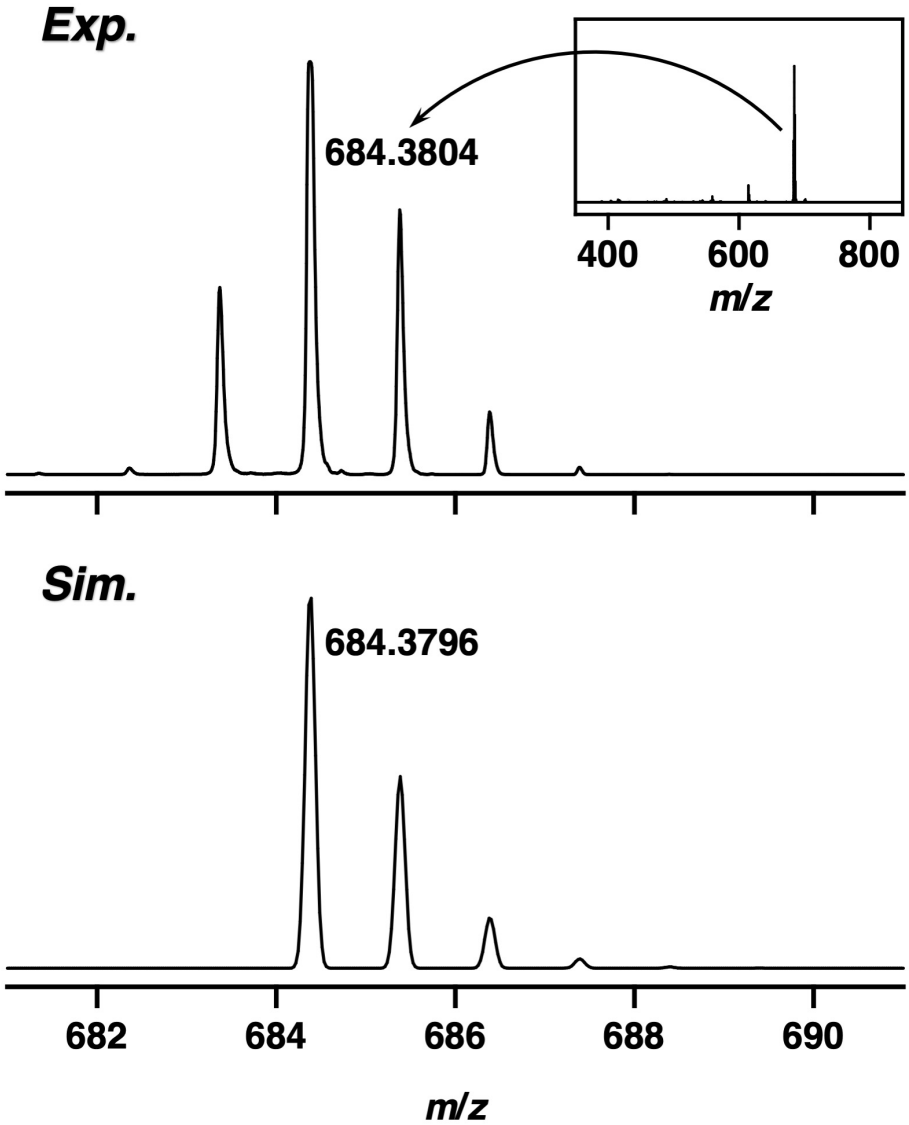

APCI TOF–MS chart of ***o*-ePDI1–DBA** (positive ion) and its calculated isotopic distribution (calcd. for $C_{44}H_{50}N_3O_4$; $[M+H]^+$). The target compoud was detected both as the positively charged ($[M]^+$) and the protonated ($[M+H]^+$) species under the measurement conditions.

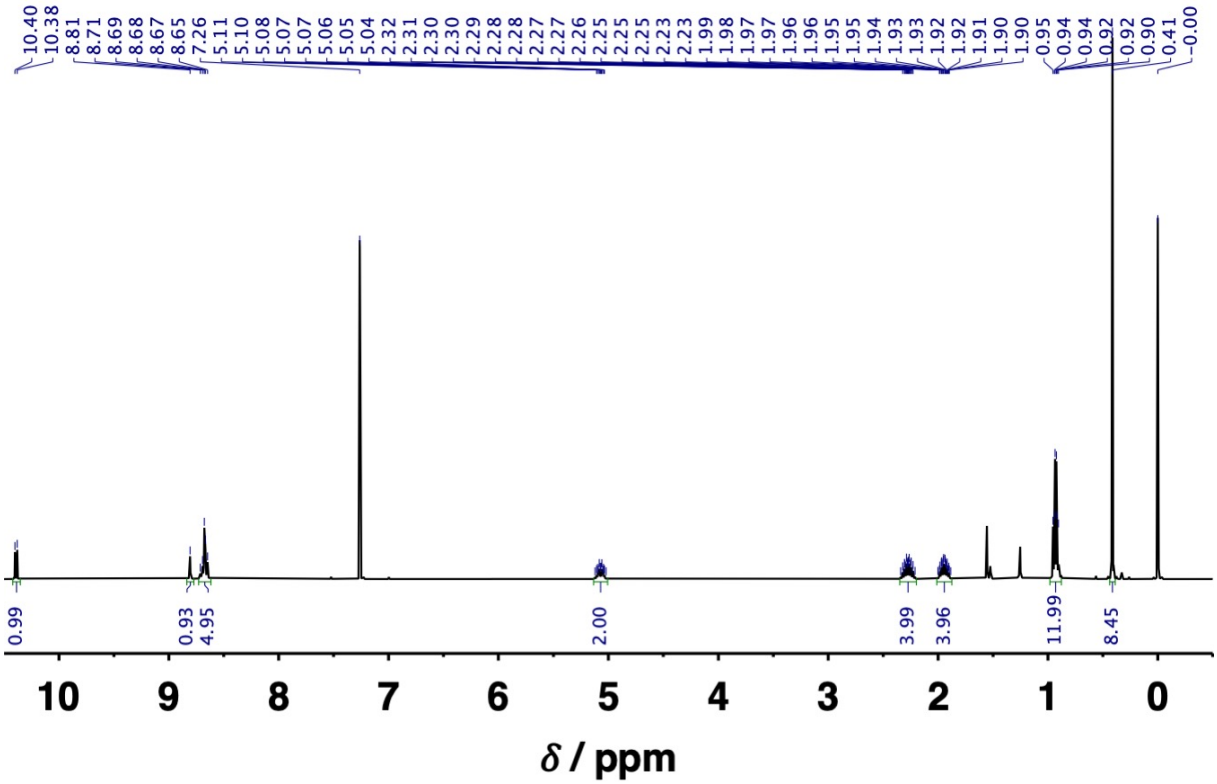

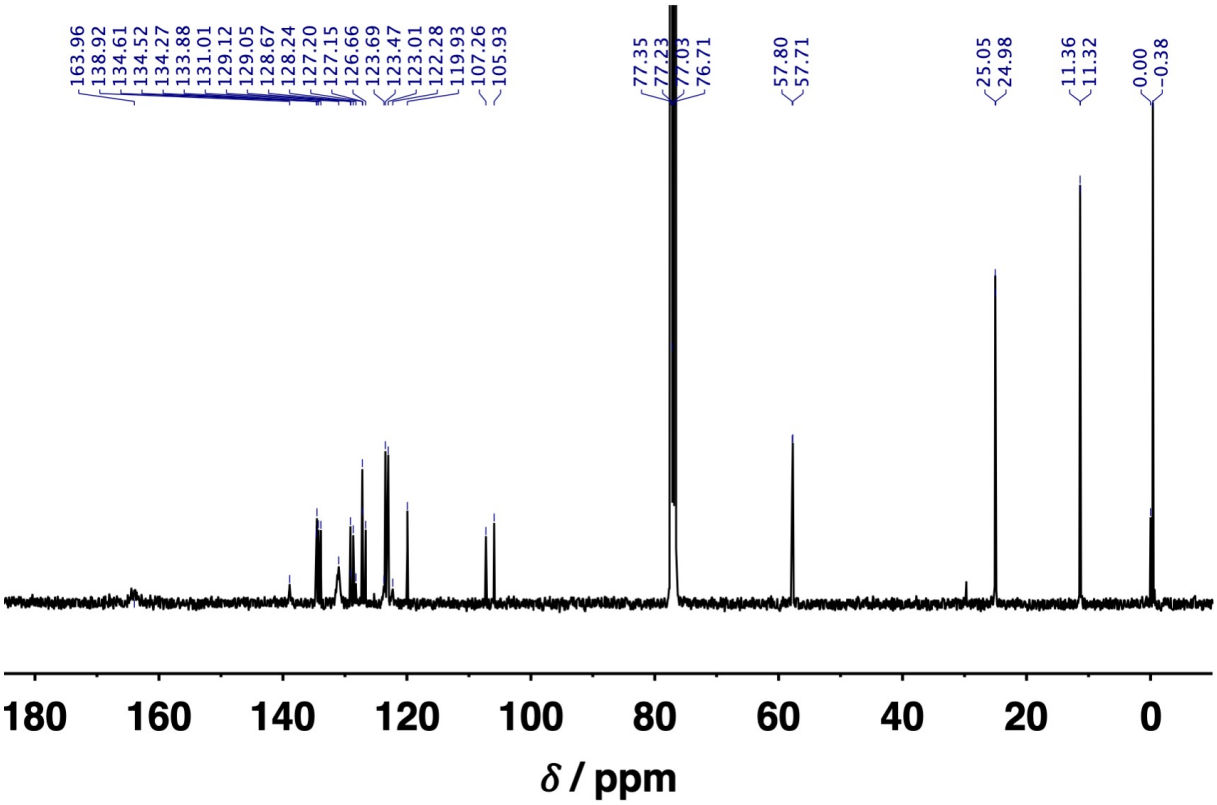

^{1}H NMR (top) and ^{13}C NMR (bottom) spectra of ***b*-ePDI1-TMS** in $CDCl_3$ at 298 K.

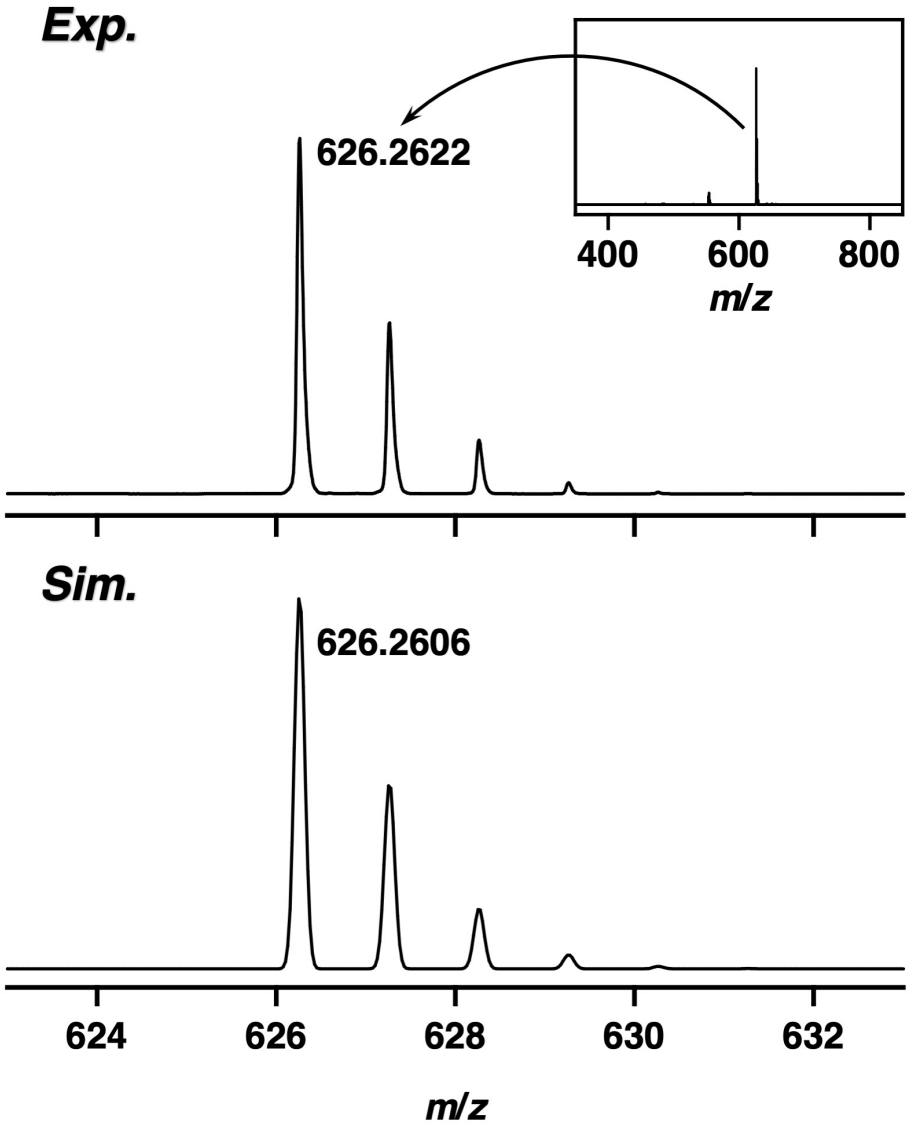

APCI TOF–MS chart of ***b*-ePDI1-TMS** (negative ion) and its calculated isotopic distribution (calcd. for $C_{39}H_{38}N_2O_4Si$; $[M]^-$).

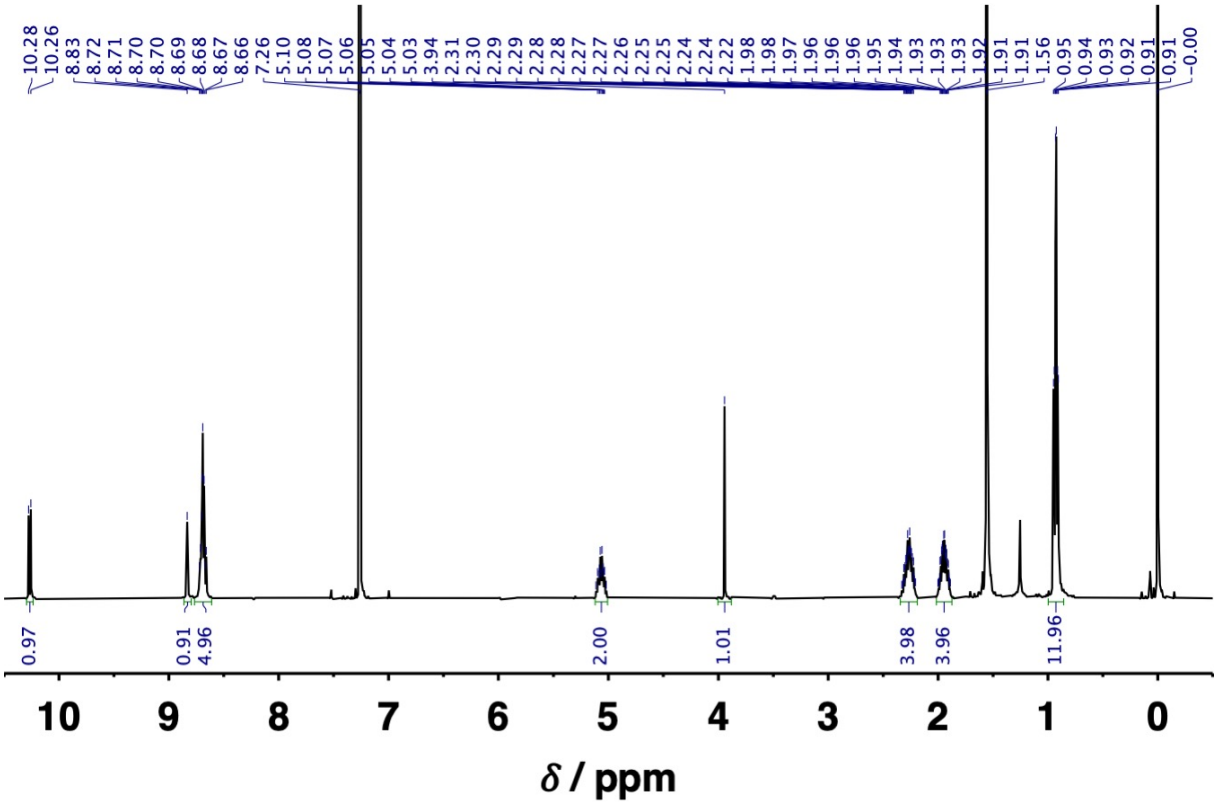

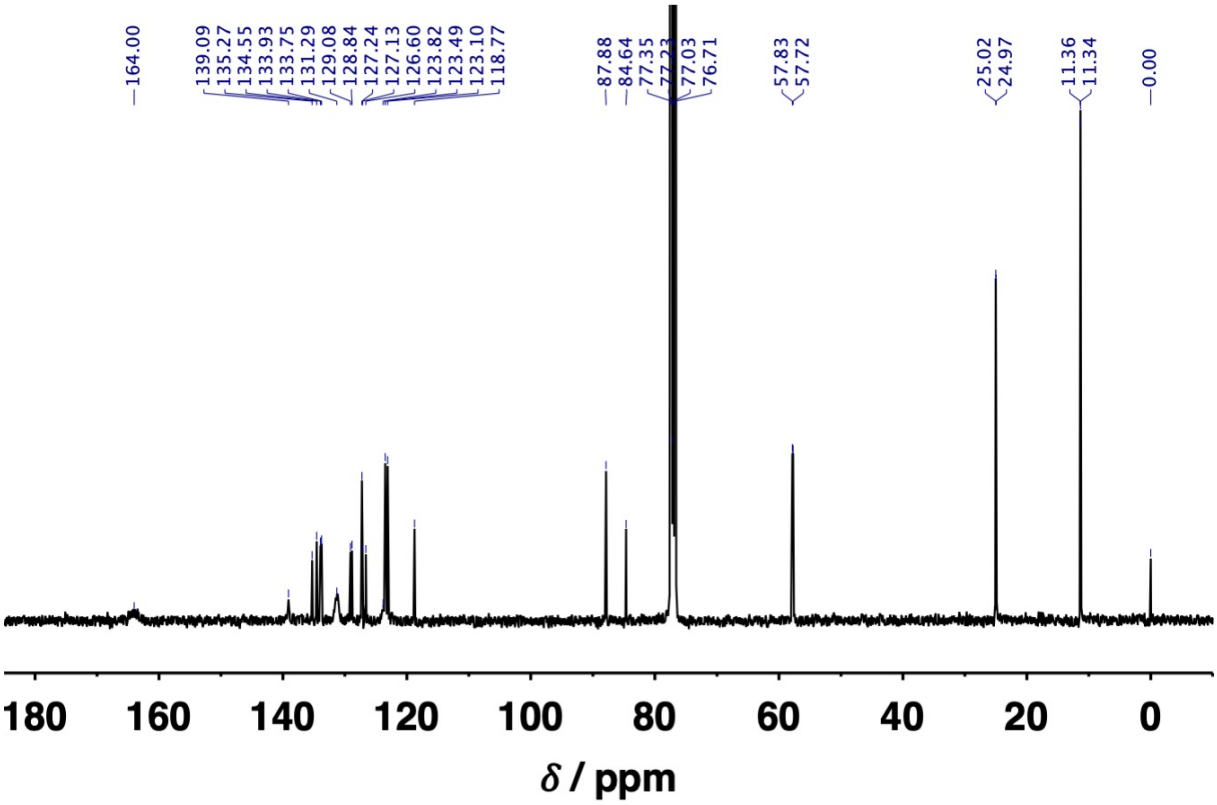

^{1}H NMR (top) and ^{13}C NMR (bottom) spectra of ***b*-ePDI1** in $CDCl_3$ at 298 K.

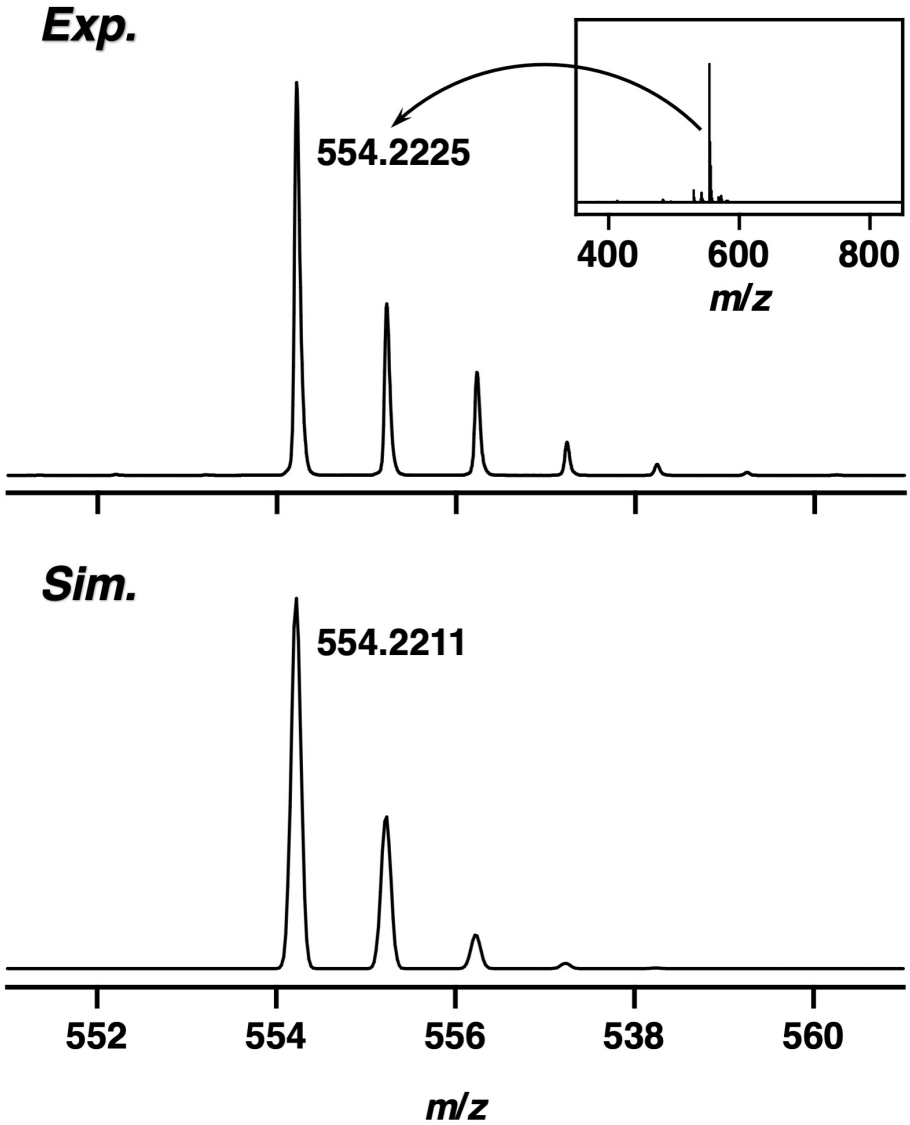

APCI TOF–MS chart of ***b*-ePDI1** (negative ion) and its calculated isotopic distribution (calcd. for $C_{36}H_{30}N_2O_4$; $[M]^-$).

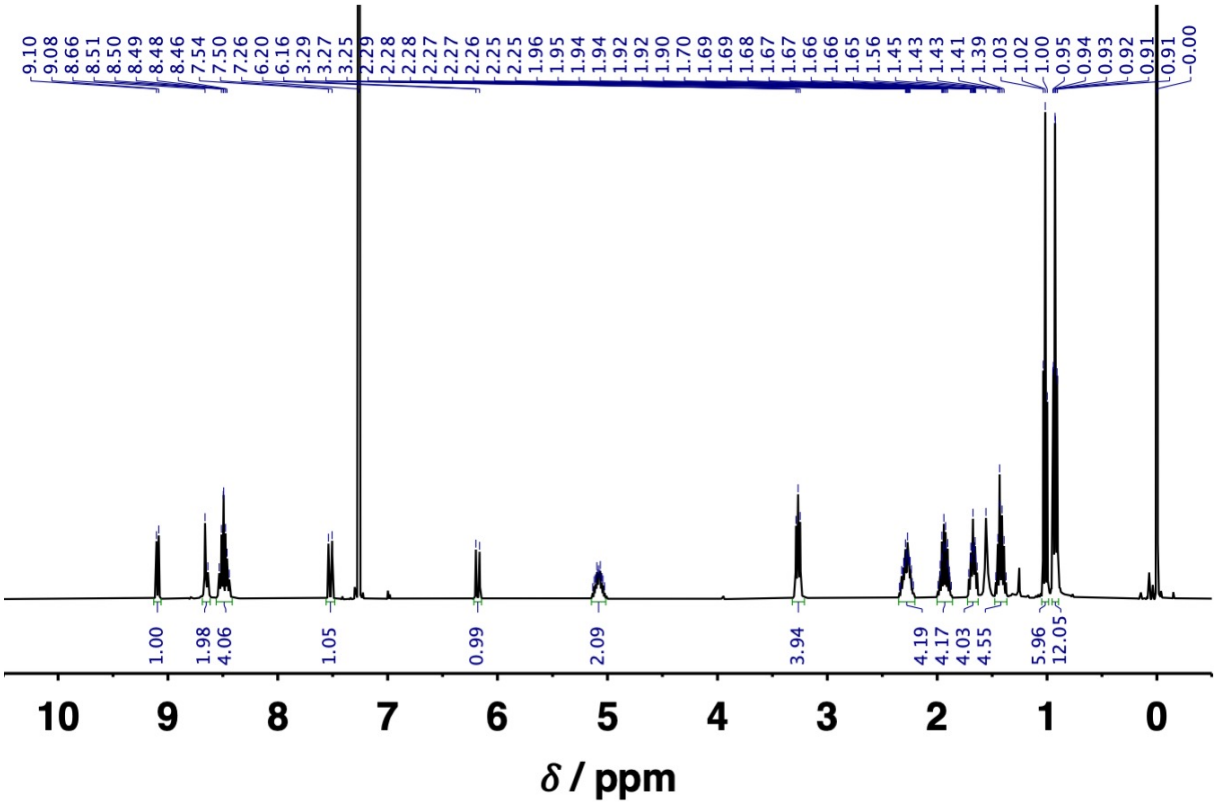

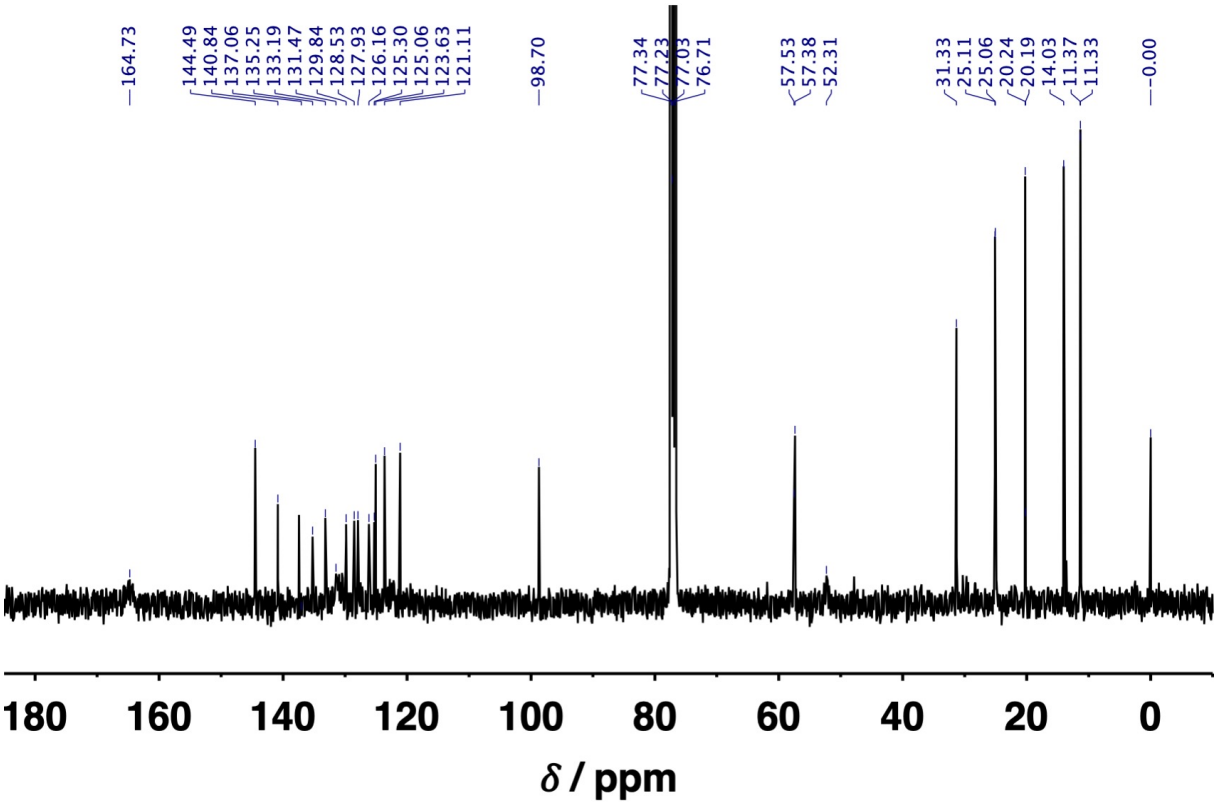

^{1}H NMR (top) and ^{13}C NMR (bottom) spectra of ***b*-ePDI1–DBA** in $CDCl_3$ at 298 K.

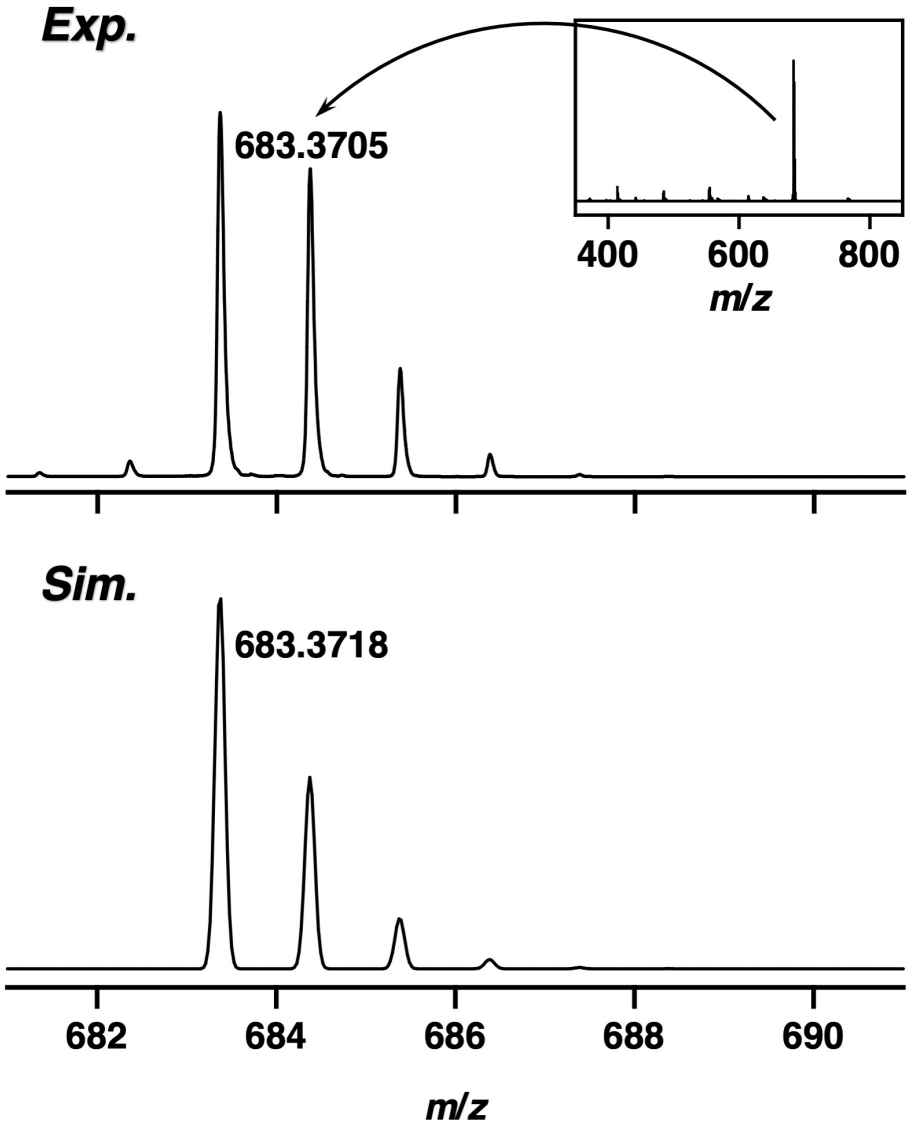

APCI TOF–MS chart of ***b*-ePDI1–DBA** (positive ion) and its calculated isotopic distribution (calcd. for $C_{44}H_{49}N_4O_4$; $[M]^+$).

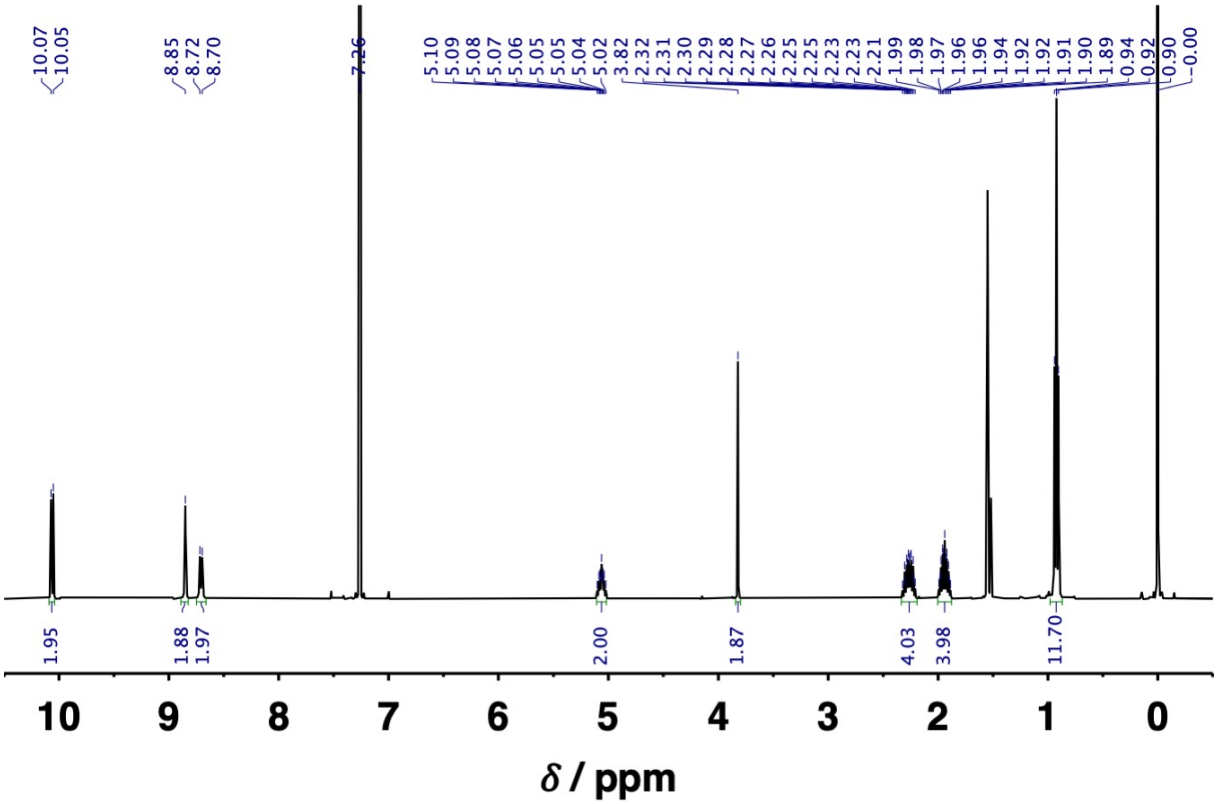

^{1}H NMR spectrum of ***b*-ePDI2** in $CDCl_3$ at 298 K. The ^{13}C NMR spectrum could not be obtained even at higher temperatures or in other solvents due to the poor solubility of ***b*-ePDI2**.

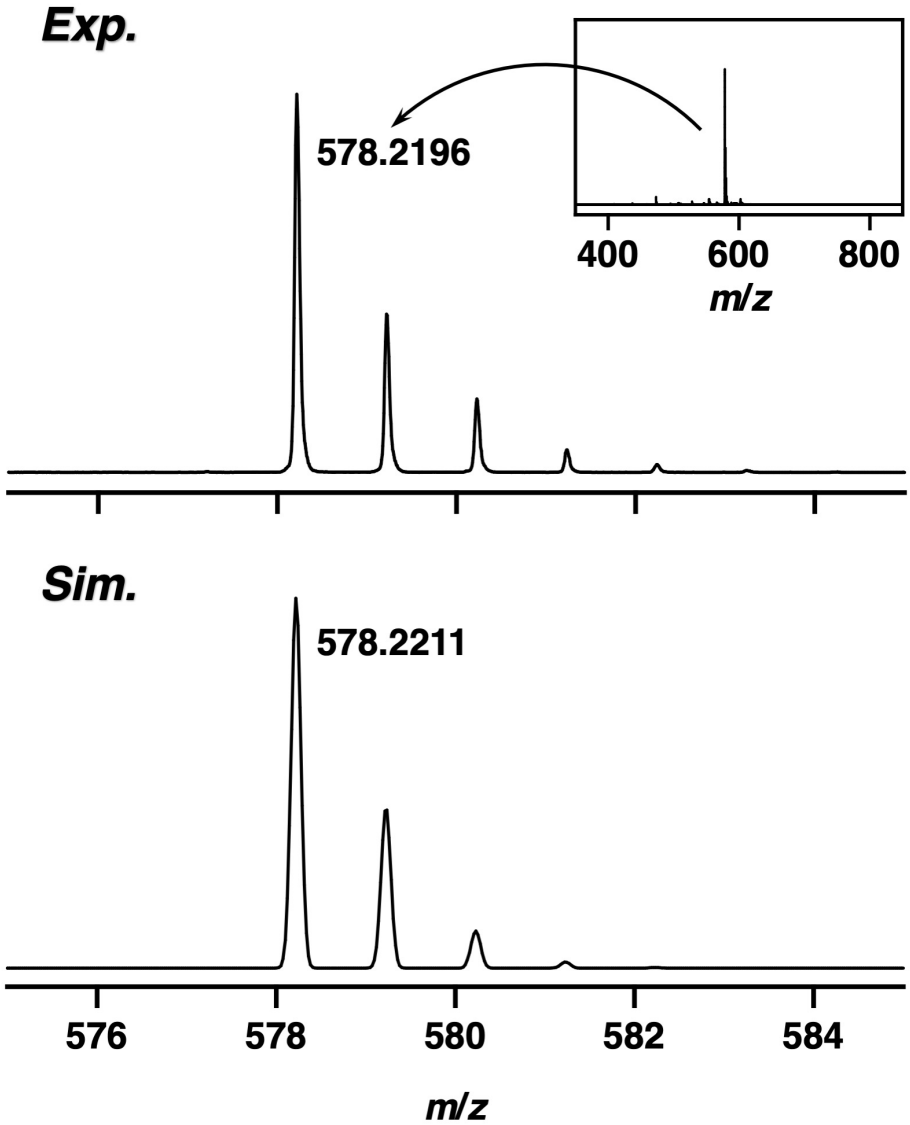

APCI TOF–MS chart of ***b*-ePDI2** (negative ion) and its calculated isotopic distribution (calcd. for $C_{38}H_{30}N_2O_4$; $[M]^-$).

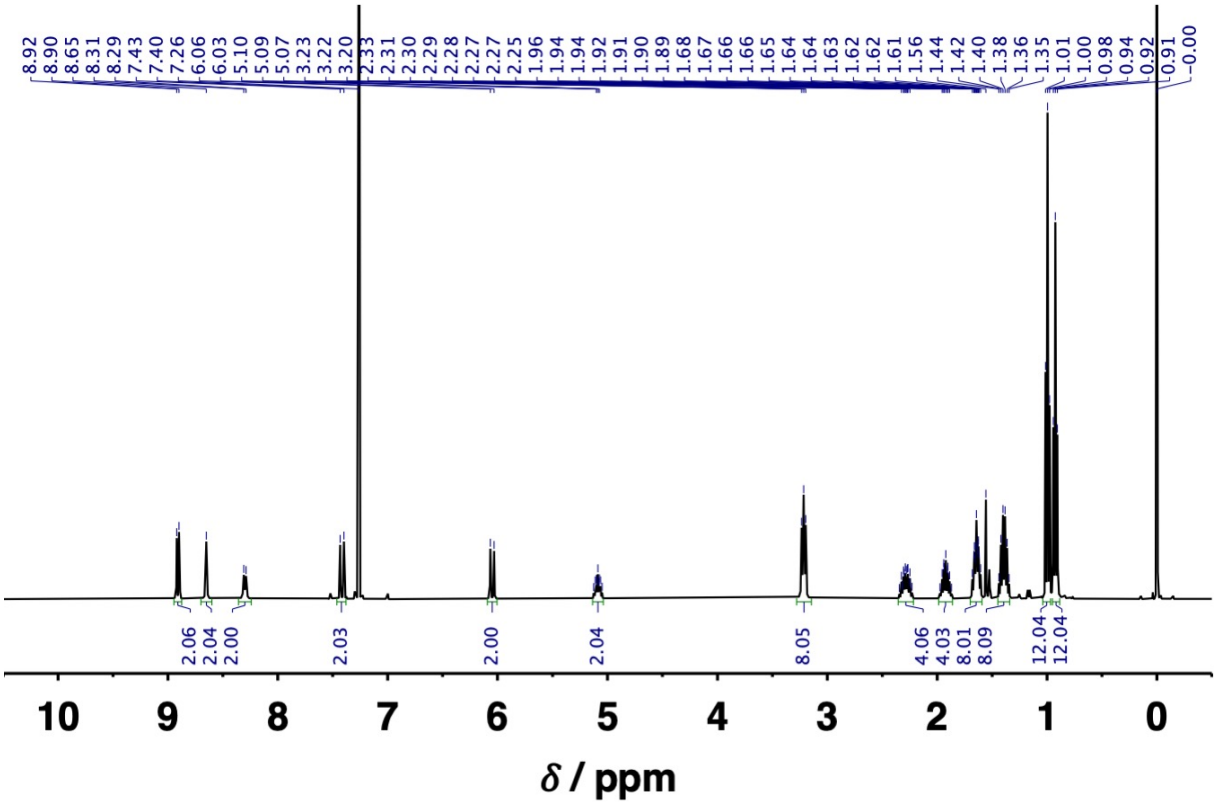

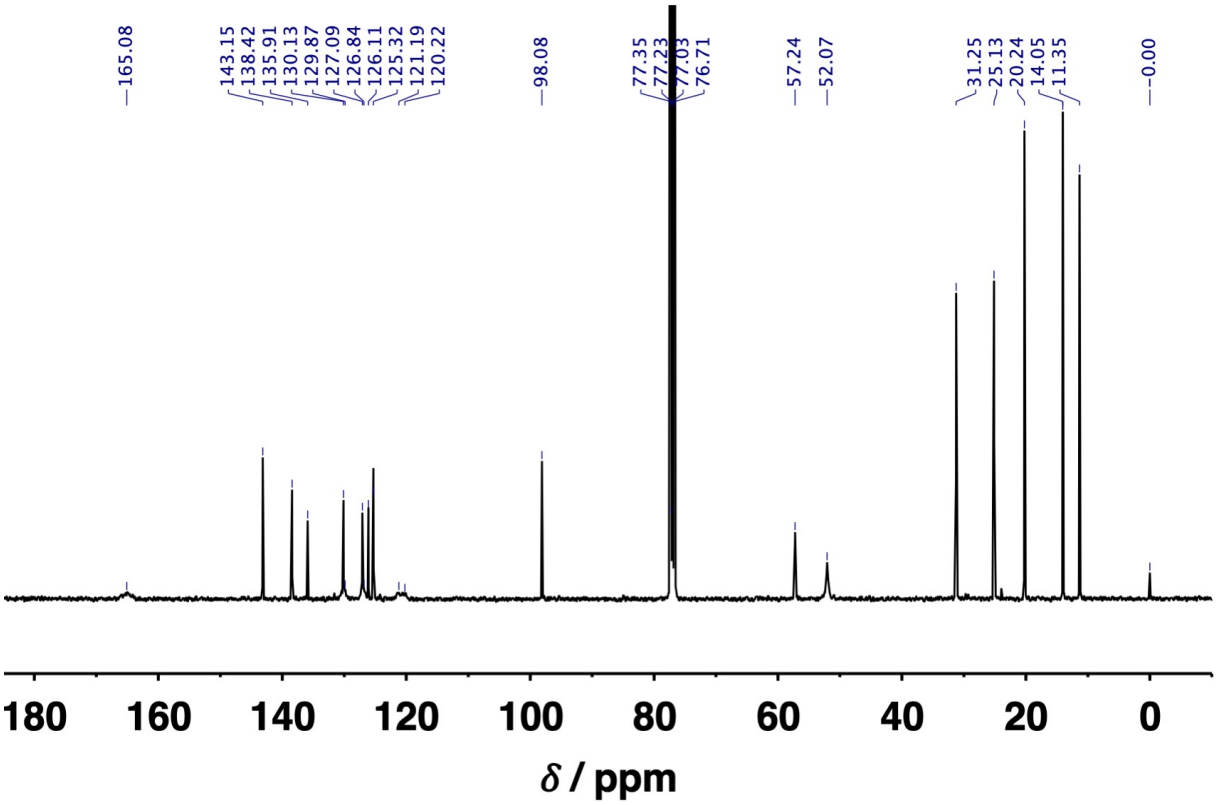

^{1}H NMR (top) and ^{13}C NMR (bottom) spectra of ***b*-ePDI2–(DBA)$_2$** in $CDCl_3$ at 298 K.

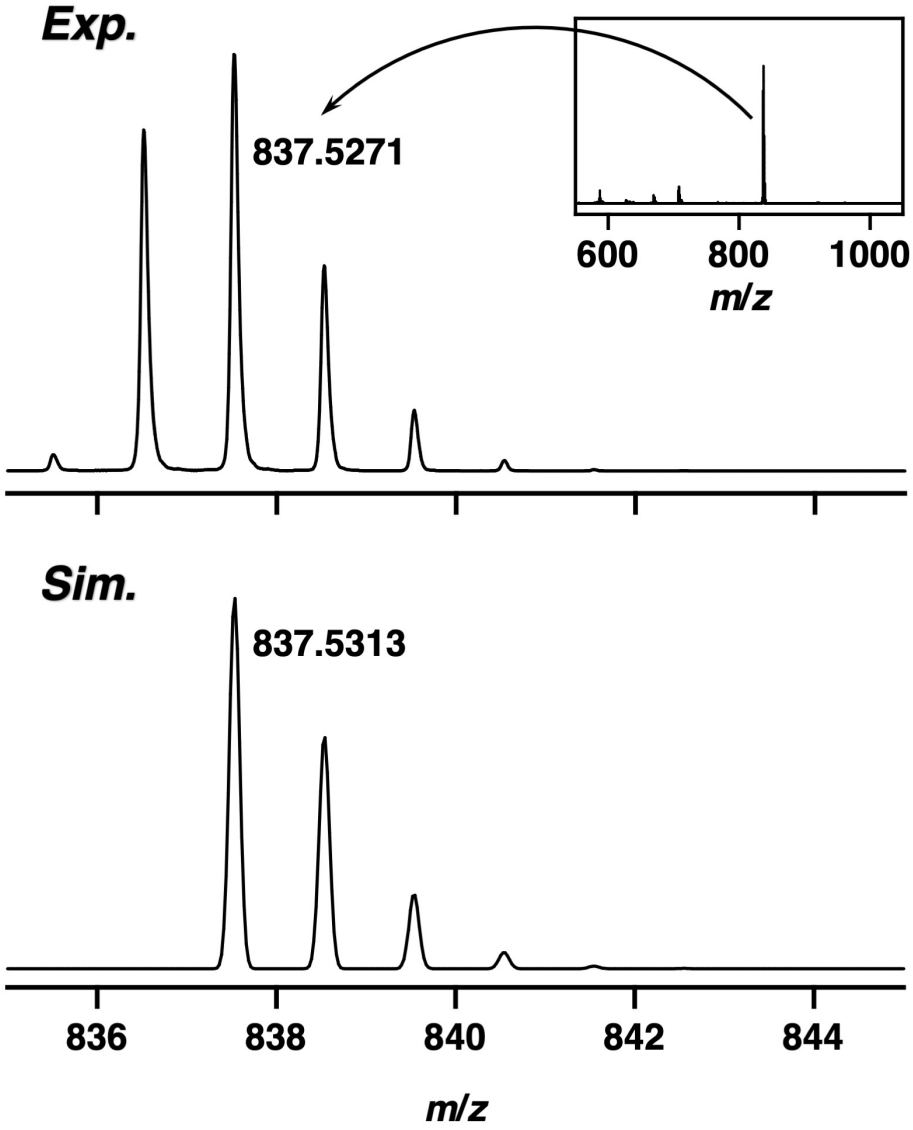

APCI TOF–MS chart of ***b*-ePDI2–(DBA)$_2$** (positive ion) and its calculated isotopic distribution (calcd. for $C_{54}H_{69}N_4O_4$; $[M+H]^+$). The target compoud was detected both as the positively charged ($[M]^+$) and the protonated ($[M+H]^+$) species under the measurement conditions.

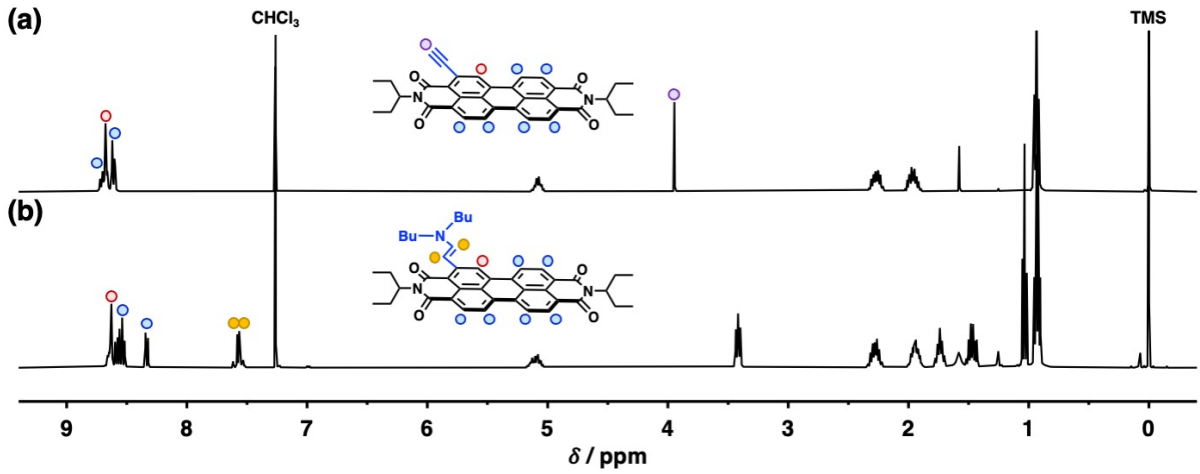

Fig. S1 ^{1}H NMR spectra of (a) ***o*-ePDI1** and (b) ***o*-ePDI1–DBA** in $CDCl_3$ at 298 K. The chemical shift of the *bay*-proton adjacent to the reaction site (red circle) of ***o*-ePDI1–DBA** was upfield shifted by 0.05 ppm. The chemical shifts of the enamine proton of ***o*-ePDI1–DBA** appeared at 7.55 ppm and 7.60 ppm with a *J* value of 13.8 Hz.

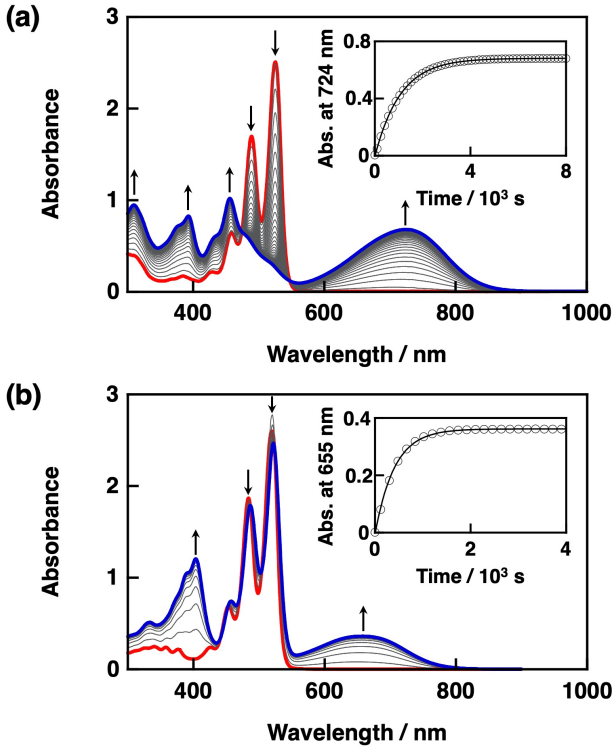

Fig. S2 UV-vis-NIR absorption spectral changes observed upon addition of **DBA** (96 mM) to a DME solution (40 μM) of (a) ***b*-ePDI1** and (b) ***o*-ePDI1** at 298 K. Each inset shows a time profile of the absorbance change at 724 nm for ***b*-ePDI1** and 655 nm for ***o*-ePDI1**, fitted by a first order kinetic curve with an R^2 value of over 0.99.[S6] The second order rate constant for the formation of ***b*-ePDI1–DBA** (9.74×10^{-3} M^{-1} s^{-1}) was 2.6-fold smaller than that of ***o*-ePDI1–DBA** (2.56×10^{-2} M^{-1} s^{-1}), maybe due to the sterically crowded ethynyl group at the *bay*-position.

The absorption band of ***b*-ePDI1** at 525 nm attributed to the π–π* transition was significantly decreased by the amino-yne click reaction, while that of ***o*-ePDI1** at 521 nm was slightly decreased, suggesting that the electron-donating character of the amine at the *ortho*-position does not affect the electronic state of the PDI π-core.

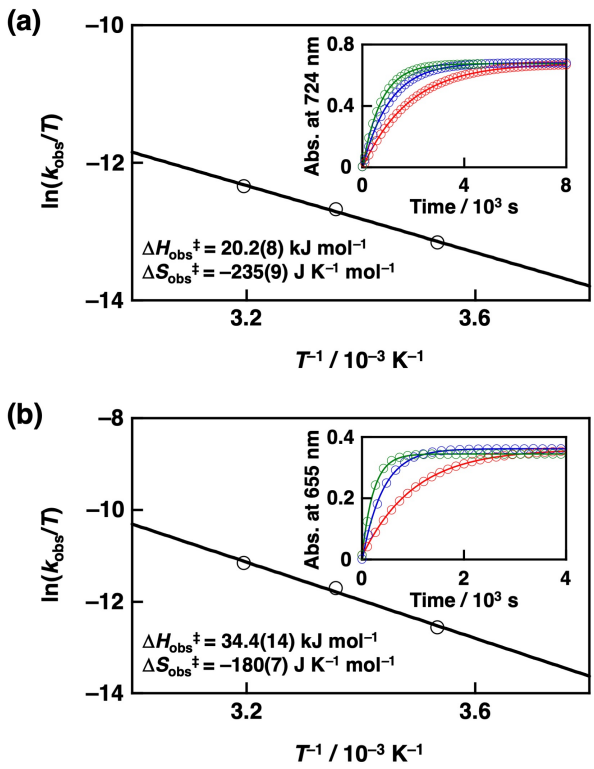

Fig. S3 Eyring plot for the reaction of (a) ***b*-ePDI1** (40 μM) and (b) ***o*-ePDI1** (40 μM) with **DBA** (96 mM) in DME. The activation enthalpy and entropy are also shown. The free energy of activation at 298 K are calculated to be 90.2(35) kJ mol^{-1} and 88.0(35) kJ mol^{-1} for the amino-yne click reaction of ***b*-ePDI1** and ***o*-ePDI1**, respectively.

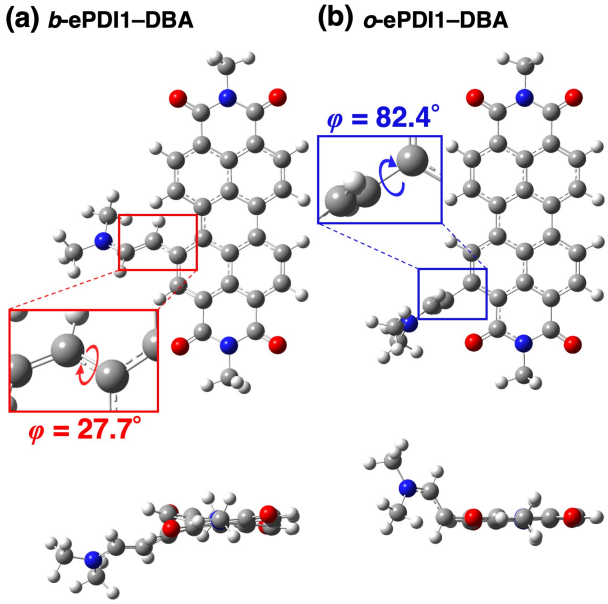

Fig. S4 Optimized structures of top (upper) and side (bottom) view of (a) ***b*-ePDI1–DBA** and (b) ***o*-ePDI1–DBA** in the singlet excited (S_1) state, calculated by TDDFT at the CAM-B3LYP/6-31+g(d) level. The butyl groups are replaced with methyl groups for simplicity. The dihedral angles (φ) between the PDI and enamine moieties are shown in the figure.

The dipole moments of ***b*-ePDI1–DBA** and ***o*-ePDI1–DBA** in the S_1 state were increased by 6.0 D and 13.9 D, respectively, compared to those in the S_0 state, suggesting the significant structural changes, especially in the case of ***o*-ePDI1–DBA**.

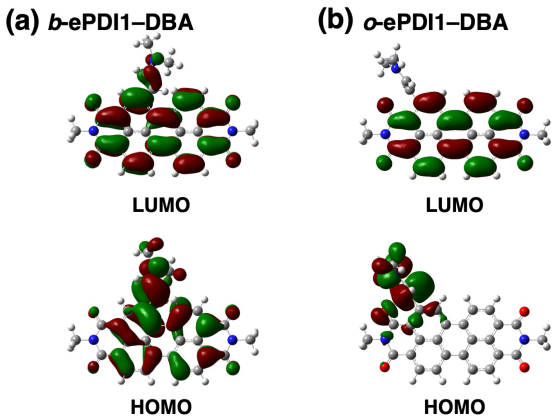

Fig. S5 HOMOs and LUMOs of (a) ***b*-ePDI1–DBA** and (b) ***o*-ePDI1–DBA** in the optimized structures in the S_1 state, calculated by TDDFT at the CAM-B3LYP/6-31+g(d) level. The butyl groups are replaced with methyl groups for simplicity. The HOMO and LUMO of ***b*-ePDI1–DBA** are delocalized over the molecule. In contrast, the HOMO and LUMO of ***o*-ePDI1–DBA** are mainly localized to the amino group and the PDI π-core, respectively.

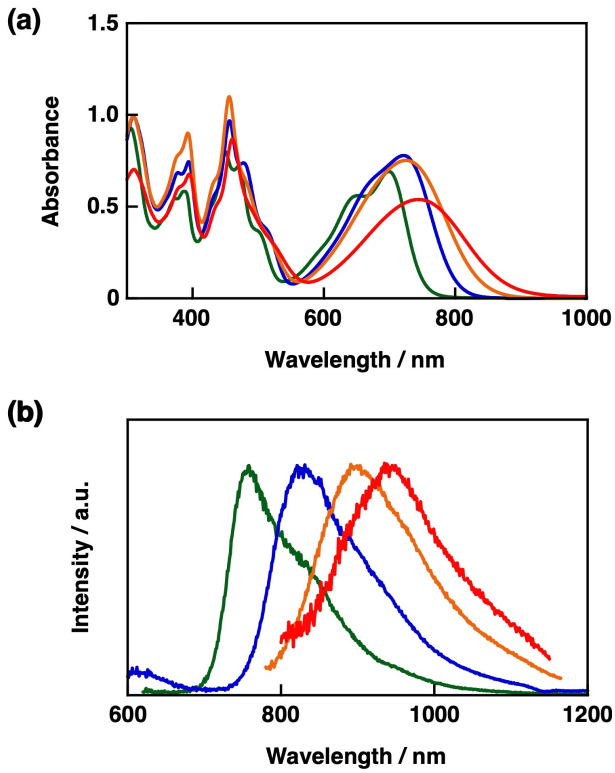

Fig. S6 UV-vis-NIR absorption (a) and normalized emission (b) spectra of ***b*-ePDI1–DBA** (40 μM) in dodecane (green), toluene (blue), DME (orange), MeOH (red) at 298 K. The emission spectra are normalized to the maximum intensity. The excitation wavelength was 470 nm.

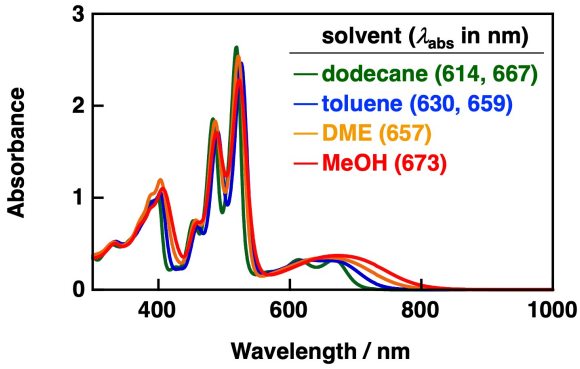

Fig. S7 UV-vis-NIR absorption spectra of ***o*-ePDI1–DBA1** (40 μM) in dodecane (green), toluene (blue), DME (orange), MeOH (red) at 298 K.

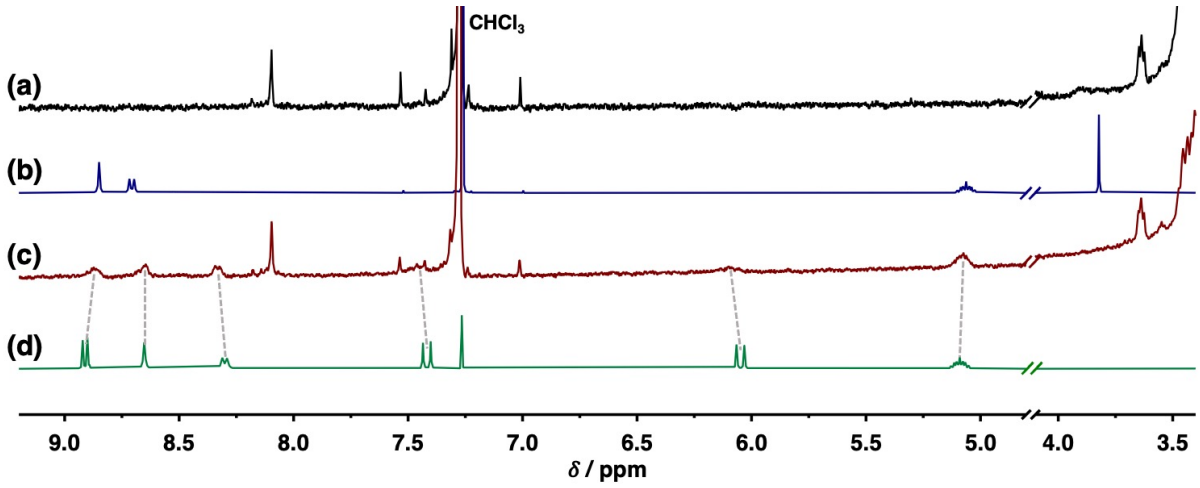

Fig. S8 ^{1}H NMR spectra of (a) **PEI**, (b) ***b*-ePDI2**, (c) ***b*-ePDI2–PEI**, and (d) ***b*-ePDI2–(DBA)$_2$** in $CDCl_3$ at 298 K.

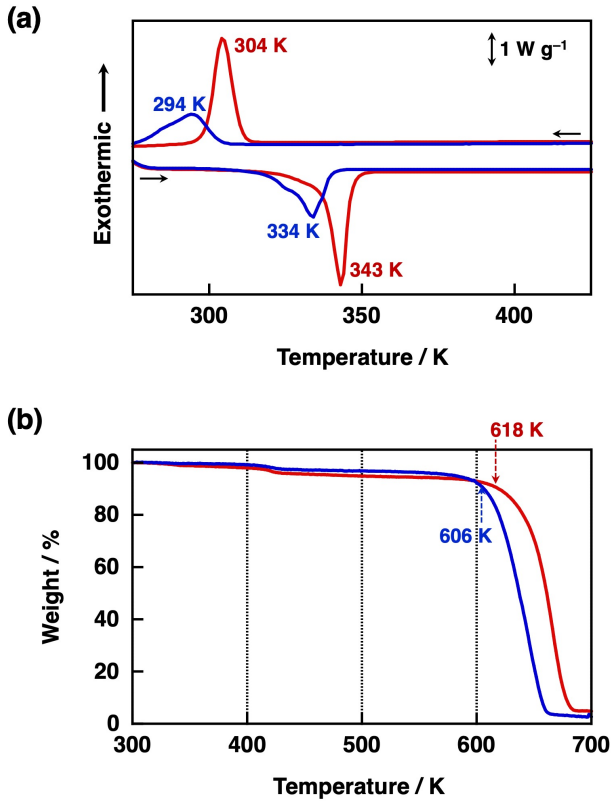

Fig. S9 (a) DSC profiles of ***b*-ePDI2–PEI** (blue) and **PEI** (red) during the second heating/cooling scan at 10 K/min. (b) TGA thermograms of ***b*-ePDI2–PEI** (blue) and **PEI** (red) under flowing nitrogen gas. The arrows indicate the temperature where 10% of the sample weight is reduced.

Supplementary References

S1. Gaussian 16, Revision C.01, M. J. Frisch, G. W. Trucks, H. B. Schlegel, G. E. Scuseria, M. A. Robb, J. R. Cheeseman, G. Scalmani, V. Barone, G. A. Petersson, H. Nakatsuji, X. Li, M. Caricato, A. V. Marenich, J. Bloino, B. G. Janesko, R. Gomperts, B. Mennucci, H. P. Hratchian, J. V. Ortiz, A. F. Izmaylov, J. L. Sonnenberg, D. Williams-Young, F. Ding, F. Lipparini, F. Egidi, J. Goings, B. Peng, A. Petrone, T. Henderson, D. Ranasinghe, V. G. Zakrzewski, J. Gao, N. Rega, G. Zheng, W. Liang, M. Hada, M. Ehara, K. Toyota, R. Fukuda, J. Hasegawa, M. Ishida, T. Nakajima, Y. Honda, O. Kitao, H. Nakai, T. Vreven, K. Throssell, J. A. Montgomery, Jr., J. E. Peralta, F. Ogliaro, M. J. Bearpark, J. J. Heyd, E. N. Brothers, K. N. Kudin, V. N. Staroverov, T. A. Keith, R. Kobayashi, J. Normand, K. Raghavachari, A. P. Rendell, J. C. Burant, S. S. Iyengar, J. Tomasi, M. Cossi, J. M. Millam, M. Klene, C. Adamo, R. Cammi, J. W. Ochterski, R. L. Martin, K. Morokuma, O. Farkas, J. B. Foresman and D. J. Fox, Gaussian, Inc., Wallingford CT, 2016.

S2. GaussView, Version 6.1, R. Dennington, T. A. Keith and J. M. Millam, Semichem Inc., Shawnee Mission, KS, 2016.

S3. (*a*) T. Teraoka, S. Hiroto and H. Shinokubo, *Org. Lett.*, 2011, **13**, 2532; (*b*) Y. Fan, K. Ziabrev, S. Zhang, B. Lin, S. Barlow and S. R. Marder, *ACS Omega*, 2017, **2**, 377; (*c*) G. Battagliarin, Y. Zhao, C. Li and K. Müllen, *Org. Lett.*, 2011, **13**, 3399.

S4. (*a)* P. Rajasingh, R. Cohen, E. Shirman, L. J. W. Shimon and B. Rybtchinski, *J. Org. Chem.*, 2007, **72**, 5973; (*b*) Y. Yang, Y. Wang, Y. Xie, T. Xiong, Z. Yuan, Y. Zhang, S. Qian and Y. Xiao, *Chem. Commun.*, 2011, **47**, 10749.

S5. (*a*) B. A. Jones, A. Facchetti, M. R. Wasielewski and T. J. Marks, *J. Am. Chem. Soc.*, 2007, **129**, 15259; (*b*) Y. Huang, L. Fu, W. Zou, F. Zhang and Z. Wei, *J. Phys. Chem. C*, 2011, **115**, 10399.

S6. A. Takai and M. Takeuchi, *Bull. Chem. Soc. Jpn.*, 2018, **91**, 44.